Student thesis series INES nr 651

Assessment of Sediment Transportation Along the Southern and Eastern Coast of Scania, Sweden

A Case Study of Storm Babet.

Yana Tremasova

2024
Department of
Physical Geography and Ecosystem Science
Lund University
Sölvegatan 12
S-223 62 Lund
Sweden

Yana Tremasova (2024).
Assessment of Sediment Transportation Along the Southern and Eastern Coast of Scania, Sweden – A Case Study of Storm Babet. (English)
Analys av Sediment Transport Längst Södra och Östra Kustområdet i Skåne, Sverige – En Fallstudie av Stormen Babet. (Swedish)
Bachelor degree thesis, 15 credits in Physical Geography and Ecosystem Analysis
Department of Physical Geography and Ecosystem Science, Lund University

Level: Bachelor of Science (BSc)

Course duration: *March* 2024 until *June* 2024

Assessment of Sediment Transportation Along the Southern and Eastern Coast of Scania, Sweden

A Case Study of Storm Babet.

Yana Tremasova

Bachelor thesis, 15 credits, in Physical Geography and Ecosystem Analysis

Supervisors:
Andreas Persson (Department of Physical Geography and Ecosystem Science),
Sebastian Bokhari Irminger (Swedish Geotechnical Institute)

Exam Committee:
Helena Elvén Eriksson,
Patrik Vestin
Department of Physical Geography and Ecosystem Science

Acknowledgements

I want to raise my acknowledgement to my supervisor Sebastian Bokhari Irminger and the Swedish Geotechnical Institute for making this project possible. Sebastian has given his support, provided new ideas and given valuable feedback throughout the entire project.
In addition, I would like to express my gratitude to my supervisor Andreas Persson for his invaluable insights on the methods and his consistent availability and support. Lastly, I would like to thank Fintan Griffin for giving me valuable tips on my methodology, Nele Noack for giving feedback on the report, as well as my other coursemates for their positivity throughout this course.

Preface

The following project is done in collaboration with Swedish Geotechnical Institute (SGI). Established in 1944, SGI is an administrative authority in Sweden focusing on ensuring safe and sustainable development. To reach the latterly mentioned objective, they aim at reducing factors such as landslides and coastal erosion. In addition, SGI also aids municipalities and external authorities with their expertise (SGI, 2023*a*). SGI is currently working on analysing the aftermath as a result of Babet. In 2023, SGI have done LiDAR scanning of the coastal area of Scania. This data, along with a LiDAR scanning from 2019 will be utilized in this study. In addition, SGI has provided the author with GPS point data transects along the coast taken before and after Babet.

Abstract

The majority of the coastal area of Scania is highly susceptible to sediment transportation. Due to various influences which are both human induced and natural, the morphology of coastal dunes often alters. Therefore, it is important to assess these changes, especially after major cyclonic storms such as the storm Babet in order to get a comprehensive understanding of the aftermath. The purpose of this study is to assess changes in sediment volume after storm Babet, conduct a map quality assessment on the data used, as well as discuss various mitigation strategies along the coastal area of 8 municipalities stretching from Vellinge to Sölvesborg.

Using GIS, Digital Elevation Models (DEMs) from 2019 and 2023 were subtracted from each other, which yielded positive (accumulation) and negative (erosion) values. These values were analyzed individually across two digitized zones that were split per municipal border - zone 1 (from dune top to dune toe) and zone 2 (from dune toe to waterline). Both zones were digitized based on images interpretation, with the help of visual data such as HillShades and numerical data such as contour lines. However, it still yields some level of subjectiveness. The study found that Ystad had the highest change in zone 1 (-4.33 m^3/m) and Bromölla the lowest (-0.01 m^3/m). In zone 2, Simrishamn had the highest change (1.53 m^3/m) and Sölvesborg the lowest (-0.16 m^3/m). These variations are influenced by factors like sand availability, strong winds, urbanization, mitigation strategies, vegetation, and soil type of the specific area. Coastal areas consisting of pebbles, and vegetation resulted in less sediment displacement than area consisting of sand grains.

A site-specific assessment was done remotely for Anton Fiskares Väg (Ystad) and Rörum (Simrishamn), with volume change calculated per 1000 square meters and visualized using Getis-Ord-Gi* HotSpot analysis. This provided a clearer picture of erosion and accumulation patterns, indicating possible causes like wind patterns, barriers such as fallen trees as a result of Babet, and tourism.

Map quality was assessed by comparing DEMs with manually collected elevation data with high-precision coordinate points. It is concluded that the accuracy varied depending on the location and the date of the manually measured RTK-GNSS points. This alternation is influenced mainly by LiDAR errors but also altering environmental factors such as tides and sediment displacement. Even though not all volume changes can be attributed solely to Babet, it remains the most significant event between 2019 and 2023, influencing the majority of the volume changes during this period. For more significant research, it was concluded that continued site-specific volume change assessments and comparisons with other methods are recommended for better dune identification and monitoring.

Keywords: *Volume Change Assessment, Storm Babet, Sediment Transportation, GIS, LiDAR*

Table of Contents

1 Introduction

The coastal area of Scania has crucial ecosystem functions in the form of dunes, vegetation, and vulnerable species. For example, dune can act as a protective barrier against storm surges and erosion, thus offering habitat for various species of flora and fauna (Sigren, et al., 2014; Provoost, et al., 2009; Debaine & Robin, 2012). Therefore, coastal dunes are generally rich in biodiversity. They also hold historical significance as the slow morphological process can tell the history of past landscapes and climate change processes (Provoost, et al., 2009). However, these features have changed more frequently since the 1900s century as a result of numerous factors, including both human-induced and natural disturbances such as storm surges. Overtime, this can make dunes unstable, decreasing their protective function and increasing sediment transportation which in turn leads to destruction of nearby settlements and ecosystems (Hesp & Martínez, 2007). Sediment transportation is a natural process that stems from erodible sediments that are exposed to the flow of fluids, such as water or air, setting bed particles into motion (Pähtz, et al., 2020). Although the process is similar to erosion, it focuses solely on movement of sediment, excluding the process of detachment and dissolution (The Geological Society, n.d.).

Storm surges and sediment transportation are expected to become a more frequent issue in the future (IPCC, 2021). This will also result in higher levels of destructiveness exhibited by cyclones, a trend researchers attribute to human-induced climate change (Eyring, et al., 2021). Numerous scenarios project a decrease in the number of storms with more intense precipitation rates whereas others project no significant change in frequency making the future uncertain (McDonald, 2011; Ranson, et al., 2014).

An example of extreme erosion of the coastal area occurred as a result of an extratropical cyclone called “Babet” that hit numerous countries during October 2023. Urban areas near the southern and southeastern coast of Sweden have been highly affected, as the sediment was transported inland (SMHI, 2023*a*). The effect of this event is still present and the assessment of it is still ongoing. Various governmental organizations and companies such as Swedish Geotechnical Institute (SGI) are collaborating on data collection in Scania, Sweden with the objective to compare the changes within the coastal area before and after Babet (SGI, 2023*b*).

As of December 2023, laser scanning of the affected coastal areas in Scania have been conducted through a collaboration with SGI, the Land Survey, Swedish Forest Agency, and the affected municipalities. The aim of the laser scanning was to gather general understanding of the aftermath and to better detect the most affected areas (SGI, 2024*a*). As of now, it can be concluded that the majority of Scania’s south- and east coast were affected by the storm, showcasing at least 0.75 m sediment loss (SGI, 2024*b*). Nevertheless, a more thorough analysis is needed to completely understand the aftermath of the storm and to compare the accuracy of the newly generated elevation data. For this reason, this project will be carried out as a

collaboration with SGI in order to assist in their ongoing efforts. Furthermore, it will emphasize the importance of enhancing preparedness to build resilience against similar events and to increase understanding of the consequences of the storm Babet.

1.1 Objectives

The primary aim of this project is to observe the sediment displacement along Scania's south- and east coast as well as assessing whether the change correlates with Babet or other factors. The secondary aim is to assess the quality of the data used in this study. Through the use of the available data, observations and analysis will be conducted through GIS.

The objectives for this study are to:

(1) Assess the sediment transportation within the beach area in m^3/m.
(2) Find municipalities with highest and lowest erosion and accumulation values.
(3) Assess the availability of the data and how it affects the outcome of coastal change analysis.

Additionally, some possible solutions for the future are discussed. These are mostly based on literature.

1.2 Hypotheses

(1) It is hypothesized that the difference between the digital elevation models from before and after Babet is the highest in municipalities already prone to sediment displacement such as Ystad and Simrishamn.
(2) Beach areas near towns or villages are assumed to be affected the most since human activities can disrupt the natural processes of dunes reducing their protective effectiveness against storms and erosion.
(3) It is expected that the coastal area in various places would experience erosion and accumulation simultaneously as the result of sediment displacement.

2 Background

2.1 Storm Babet

During the span of 18-21st of October 2023, various parts of northern and Western Europe, including the UK, Germany, Denmark, and Sweden, experienced an intense extratropical cyclone storm named "Babet". This cyclone originated from the southeast of the Atlantic Ocean (SMHI, 2023*a*). An extratropical cyclone can be defined as a cyclonic storm that forms in the mid-latitudes in both hemispheres. It is the result of polar front jet stream and baroclinic instability, which is the instability between the warm and cold air (Ahrens & Henson, 2018).

The storm can bring heavy precipitation and winds, as well as sea level fluctuations, attributed to pressure differences, wind, and intensive waves (Olaoluwa, et al., 2022).

Babet was energized by a strong jet stream as well as the warm sea surface temperatures from the Atlantic Ocean (Kendon, 2023). Consequently, it caused a rising of sea levels and strong wind gusts (SMHI, 2023*a*; Kendon, 2023). For example, Denmark reported a water level rise of up to two meters above mean sea level in various coastal areas, such as southern Little Belt and Jutland fjords. This has marked Babet as the most violent storm in over 100 years in the country (Brandt, 2023). Similarly in Sweden, the aftermath of the storm led to sea levels exceeding 1 m above mean sea level, as observed in Simrishamn municipality where the water rose to 1.26 m, causing damage to sections of the infrastructure (SMHI, 2023*b*). Overall, the sea level rise has led to considerable erosion damage in the coastal regions of Scania, impacting nearby settlements and land along the affected areas.

2.2 Sediment Transportation

As mentioned in chapter 1, sediment transportation involves the erosion of sediment from one location and its subsequent accumulation in another. In order for sediment transportation to occur, the exerted shear stress by the fluids must exceed the threshold shear stress of the sediment (Pähtz, et al., 2020; Huertos, 2020). Factors such as grain size, density, and the morphology of the particles can also determine the sediments susceptibility to erosion. For instance, fine sediments tend to suspend in the water for longer periods and are therefore more susceptible to displacement than coarser sediments (Huertos, 2020; Costa, 2016). These factors, along with the velocity rate and depth of water, determine whether the sediment will be transported as bedload or suspended load (Turowski, et al., 2010; Fondriest Environmental Inc, 2014). Generally, denser sediments tend to be transported through bedload. This means that they are set into motion through rolling and sliding along the channel bed. On the contrary, lighter particles that are transported as suspended load are buoyed by turbulent forces, allowing them to travel longer distances without adhering to the channel bed (Turowski, et al.,2010; Fondriest Environmental Inc, 2014; Costa, 2016).

Different environments may also influence the rate of erosion and transportation. In marine areas for example, transportation is often driven by tides, surges, or waves whereas in terrestrial environments, factors such as gravity and wind are the main contributors (Costa, 2016; Mitchell, 2020). In addition to this, the susceptibility of erosion is influenced by the sediment's placement. Sediments situated near barriers such as pebbles, bigger rocks, or vegetation result in lower rates of erosion and transportation as they slow down the process. In contrast, open landscapes with no barriers make the sediment less resilient (Sigren, et al., 2014). Moreover, due to gravity, sediment situated on steeper hillslopes is more prone to displacement compared to sediment located in gentle hillslopes (Attal, et al., 2014). Sediment transportation rate is also linked to anthropogenic factors. Land cover changes have played a significant role

in shaping coastal dunes throughout the centuries. This has led to alterations in soil characteristics, vegetation, and ecosystem dynamics (Provoost, et al., 2009). This alternation can make dunes more susceptible to sediment transportation as they disrupt the natural processes. This disruption can gradually lower dunes effectiveness in storm protection (Martínez, et al., 2013).

2.2.1 Coastal Dunes

Coastal dunes, or *sand dunes*, are sedimentary structures situated at the interface of land and ocean and can be a result of erosion. In the coasts of Scania, the dunes have a high variety, ranging from being exposed nearer to the waterline to being fully vegetated with mosses and lichens further away (Sandlife, n.d.). The structure of the dunes is generally shaped though geological processes over centuries, tracing them back to past landscape dynamics and climate change processes (Provoost, et al., 2009). This slow process is a result of repeated deposition of sediment grains over an obstacle, such as sea vegetation and litter, causing the wind or water velocity to decrease. This gradually results in grain accumulation and eventual formation of dunes (Costa, 2016). Coastal dunes are often characterized by layers of sediments with larger grain sizes which are inclined in the downstream direction, showcasing the deposition (Costa, 2016). Further, they vary in shape, size, and vegetation cover depending on their location and their morphological processes. For example, dunes situated on the backshore are formed through aeolian processes while dunes situated in coastal areas are formed through erosion (Martínez, et al., 2013). The linear ridge situated parallel along the coastal area is called a foredune and can range from 1 up to 20 meters, depending on the surrounding factors such as wind (Hesp & Martínez, 2007).

Normally, dunes can act as a buffer against stormy conditions. However, during intense storms, dunes are susceptible to erosion and sediment displacement due to increased water level and intensity of waves. Consequently, this can result in flattening of dunes, displacing the sediments offshore, alongshore, or inland, causing a risk to the nearby infrastructure. This process can be further intensified near urban areas as increased urbanization diminishes the dunes' capacity to shield against storm impacts (Martínez, et al., 2013). Dunes' vulnerability to erosion does not only damage infrastructure settlements, but also nearby ecosystems and plant species. Slight disturbances on a foredune can result in dieback of plants, whilst moderate disturbance can remove vegetational zones and severe disturbance can result in erosion, consequently rearranging species' geographical position (Hesp & Martínez, 2007).

2.2.2 Ongoing Mitigation and Adaptation Strategies Against Storm Surges and Erosion

Nature-Based Solutions

One of the most emphasized strategies against storm surges and erosion is dune restoration. This involves reshaping of the dunes, restoring natural sediment dynamics as well as vegetating the dunes which hinders the erosion process. Reshaping of dunes can be achieved by constructing fences along the backshore, which can retain wind-blown sand and facilitate the gradual formation of foredunes (Martínez, et al., 2013; U.S Climate Resilience Toolkit, 2024). Alternatively, sediment can be transferred from the shoreline plane into the foredune. Other strategies include modification of the pathways to the beach so that they are angled rather than perpendicular (Martínez, et al., 2013; U.S Climate Resilience Toolkit, 2024).

Strategies revolving vegetational restoration involve dune planting. New roots from native species can trap the wind-blown sand eventually leading to dune formation (State of Florida, n.d). Locally, Ystad Municipality is implementing nature-based solutions such as planting vegetation, re-creation of sand dunes by reshaping and fencing, as well as adding beach nourishments. Beach nourishment, which is the process of adding sand to the beach, helps maintain the shoreline and increases sediment availability. This ongoing project, done near Sandskogen and Löderups coastal area, has proven to be successful in achieving its goals (Ystad Kommun, 2024; Österlen Syd, n.d.). Post Babet, Kristianstad Municipality has also started planning on beach nourishment near Åhus, located southeast of Kristianstad city center (Kristianstads Kommun, 2024).

Gray Infrastructure

Additional approaches aim to directly address the storm surges themselves. This can involve the alternation of the environment with the help of physical structures such as storm surge barriers or seawalls. The seawalls can protect the coastal area against storm surges and floods (Horn, 2015; Mendelsohn & Zheng, 2020; Siegel, 2020). However, this approach comes with high costs in regard to both construction and maintenance (Mendelsohn & Zheng, 2020). Seawalls can come in a variety of forms and sizes, everything including concrete to brick structures with heights ranging from five up to ten meters. The structure depends mainly on local conditions such as wave height and wind speed (Siegel, 2020).

Alternative solutions include human-made dikes. They are typically built with material such as sandy clay with a seaward slope which reduces wave action and erosion on the low-lying areas (Siegel, 2020; RISC-KIT, n.d.). Hillblocks, which are alternative methods for sea dikes, can also prevent flooding events. This new method is constructed with concrete blocks with unique shapes that can reduce the wave impact on dikes. Hillblocks is becoming a recognizable method, currently employed in different countries such as the Netherlands and the United Kingdom (Siegel, 2020).

Gray infrastructure is currently being implemented in various locations within the study area. For instance, Falsterbo, located in the southeastern part of the study area, is undergoing construction of a sea-dike measuring 3 meters in height above sea level. The purpose of the dike will be to protect Falsterbo from future sea level rise and prevent damage from cyclones,

like Babet (Vellinge Kommun, 2019). Similarly, Trelleborg municipality is currently developing a smaller dike system in the western area that will reach up to 1.5 m in height above ground. Areas near other coastal settlements will also be investigated (Trelleborgs Kommun, 2023*a*). In Ystad, gray infrastructure such as piers, dikes, breakwaters are used as well with the purpose of preventing erosion risks. This has resulted in decreased erosion within the protected areas, but increased erosion outside of the protective areas (Ystad Kommun, 2024).

Soft Strategies

Other strategies involve the modification of human behavior, such as for example implementation of early warning systems, which can enhance preparedness (ISO, 2022). An example of this can be shown in 2013 when the United Kingdom experienced a large storm surge but did not suffer any significant damages due to the increased defense system. As a result, over 10 000 homes were evacuated in Eastern England. This was thanks to the early warning system called “UK Coastal Monitoring and Forecasting Service ", (UKCMF) (Horn, 2015). In addition to this, it is also crucial to mention the importance of shelters and evacuation plans in order to reduce mortality rate during cyclonic events. This, in combination with early warning systems, has been proven to be effective worldwide (Horn, 2015).

Other soft strategies include spreading awareness, collaborations, and including adaptation into policies (ISO, 2022; Climate ADAPT, n.d). An example of this is municipalities such as Trelleborg which have released information to affected property owners and are updating them about further actions after the storm Babet (Trelleborgs Kommun, 2023*c*). Furthermore, Trelleborg is monitoring the coastal area and conducting various risk assessments regularly against various future scenarios (Trelleborgs Kommun, 2023*b*). Similarly, Simrishamn has undergone risk assessments in the purpose of improving the resilience of settlements and removing various parts of infrastructure such as stairs and activity areas near the coastal area (Simrishamn Kommun, 2024*a*). Lastly, soft strategies also aim at enhancing effective urban planning (ISO, 2022; Climate ADAPT, n.d.). An example of effective urban planning can be the implementation of beach drainage systems which can lower the ground water table beneath the beach area through the installment of buried drains. The lowered groundwater can in turn create a thick layer of dried sand, which can hinder wave’s ability to displace sediments (Fischione, et al., 2022).

2.3 Theory Behind Coastal Monitoring Through GIS

As mentioned in section 2.2.1, coastal dunes can contribute to significant destruction of nearby settlements and ecosystems. The morphological alterations are often intense and heavenly influenced by the weather conditions as well as waves and tides (Lysko, et al., 2023). For this reason, monitoring morphological changes on the sand dunes is of utmost importance. This is normally done using various methods including both ground measurements through the use of

GPS, as well as remote sensing methods. These normally include the use of LiDAR (Light Detection and Ranging) scanning or drone capturing which provide aerial imagery. In addition, coastal areas can be measured from space, which provides satellite data. Satellites such as Earth Observation Satellite can obtain coastal elevation data which can be analyzed for a larger scale. In contrast, LiDAR data utilizes light from a pulsed laser in combination with other data such as GPS-data points, in order to provide a three-dimensional image of the Earth, showcasing the topography. Since LiDAR data is often collected from airplanes and helicopters, it can be used for smaller scaled analysis (NOAA, 2023). If one wants to gather a visual representation of the area, aerial images and orthophotos can provide a bird-eye view of the desired area on a small scale, depending on whether the image is taken from an airplane, helicopter, or a drone. However, the difference is that orthophotos have a uniform scale as the effect of tilt is removed in comparison to aerial photography, minimizing distortions and showcasing the true proportions of site (USGS, n.d.). Whether to utilize ground measurements, satellite, or aerial based images depends on the scale of the study area as well as the aim. This is due to there being advantages as well as disadvantages for all the latterly mentioned methods. The higher the image is taken above the ground, the greater its susceptibility to atmospheric scattering and distortions, which hinders image interpretation (Joshi, et al., 2020).

The most common way to monitor coastal morphological changes is to gather ground data GPS measurements as well as digital elevation models of the desired area. These are mostly acquired through LiDAR scanning, from which point-cloud data can be converted into DEM. For example, a study done by Doyle & Woodroffe, (2018) identified dunes utilizing LiDAR data within the south-east Australian coast. The LiDAR data underwent classification into multiple layers and was transformed into a TIN surface, revealing terrain details which in turn facilitated the identification of features such as dunes. Furthermore, aerial imagery complemented this process, further facilitated the identification of dunes.

On the other hand, there are several difficulties regarding remotely assessing coastal changes that should be noted. Various factors, including time of day, cloud cover, wind, season, and tides hinder correct interpretation of the data (Lysko, et al., 2023). For example, cloud cover can impede the scanning process by absorbing incoming light. Furthermore, factors such as shadows, commonly cast during the afternoon, can obscure the interpretation of affected areas. Further is elaborated in the “discussions” chapter 5.

3 Materials and Methodology

3.1 The Study Area

The coastal area, located in Scania, southern Sweden, stretches from the county border of Scania/Blekinge down to Falsterbo and is approximately 250 km long. It includes 8 municipalities in total including Vellinge, Trelleborg, Skurup, Ystad, Simrishamn, Kristianstad,

Bromölla, and Sölvesborg (see fig 1). The elevation ranges between 0 to 50 meters within the study area. Moreover, the climate is shaped by both coastal and inland influences, characterized by strong winds, little precipitation, and temperature variations (Persson, et al., 2012).

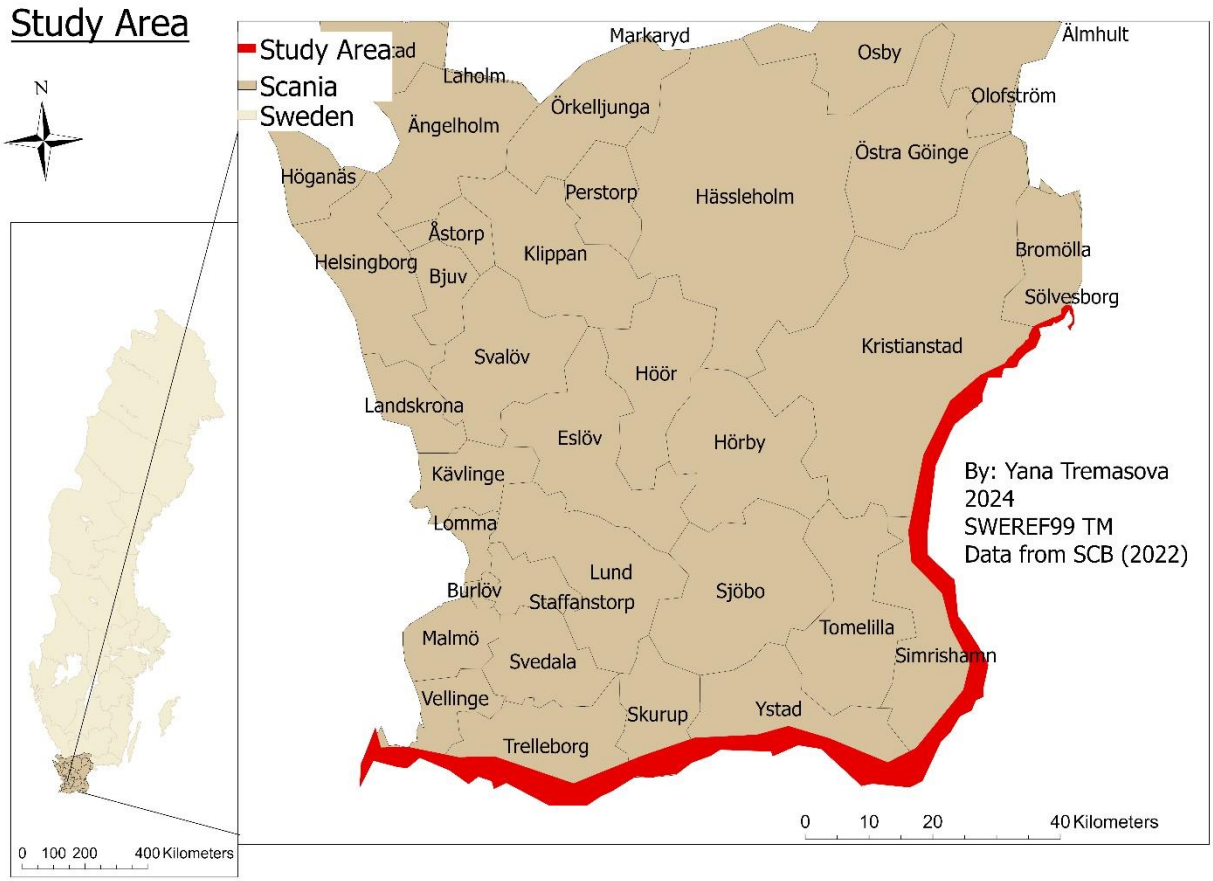

Figure 1: The study area showcased by the red polygon. It should be clarified that the study area is not fully representative of its true size.

The majority of the soil type within the coastal area of Scania consists of postglacial sand. However, there are small occurrences of glaciolacustrine sediments, particularly in areas above Simrishamn, as well as glaciofluvial sediments in Hammar, located outside of Ystad (Esko, et al., 2000). Typically, postglacial sand are deposits characterized by different layers showcasing the result of various processes, such as for instance aeolian, fluvial and glaciofluvial (Shinn, et al., 2007). The formation is influenced by external factors such as sediment supply and sea-level changes, and climate (Shinn, et al., 2007). Postglacial sand within the study area typically consists of swell-sediments formed as a result from sea-level changes. In addition, some of these sediments consist of gravel and pebbles (Esko, et al., 2000; Ising, 2022). Moreover, glaciolacustrine sediments, caused by lacustrine processes, primarily consist of fine to medium sand grains (Esko, et al., 2000). Lastly, glaciofluvial sediments consist of sand, gravel, and stones which are deposited as eskers and deltas (Esko, et al., 2000; Ising, 2022). The susceptibility towards erosion and sediment transportation depends on the grain size, soil type, and whether the shoreline mainly consists of pebbles or sand (Ising, 2022). Fig. 2

illustrates that the entire area is prone to erosion, with minor hotspots above Simrishamn, near Ystad municipality, and Falsterbo, showcasing very high susceptibility to significant erosion in loose soil layers. Fig. 2, acquired from SGU, is based on combined estimations from various data and expert assessments (SGU, 2020).

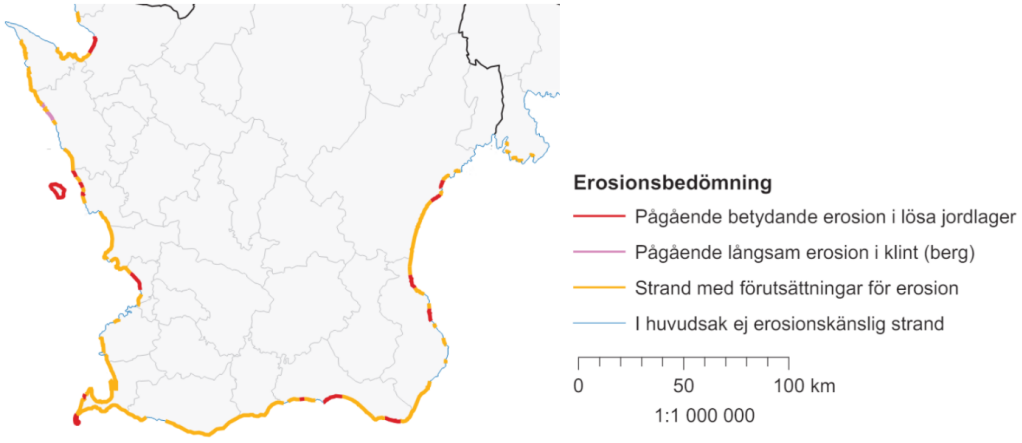

Figure 2: Coastal areas susceptibility to erosion in Scania, Sweden. Blue line showcases area not susceptible to erosion, yellow line showcases beach with conditions conductive to erosion, purple line showcases ongoing slow erosion on cliff areas and red line showcases ongoing erosion in loose soil layers. Map acquired from Swedish Geological Survey (SGU), 2020.

The land cover near the coastal study area is diverse and varies from urban to forested areas, as well as open landscapes. The most predominant land cover type is “open landscape with vegetation”, however forested areas classified as mixed and deciduous forest can also be observed. Additionally, due to the presence of several towns and settlements within the study area, urban areas are also identifiable (Naturvårdsverket, 2023).

3.2 Materials

3.2.1 Data

The following data was used in the analysis. Majority of the data below is provided by SGI, but some data was also downloaded from Lantmäteriet.

- *Real time kinematic- global navigation satellite system (RTK-GNSS) points with x, y, and z coordinates from years 2021-2023. Provided by SGI.*
- *Digital Elevation Model of 1x1 m resolution based on LiDAR data from the year 2019 (before Babet) and 2023 (after Babet). Provided by SGI.*
- *Aerial orthophotos with 25 m resolution from year 2022 made by Lantmäteriet, acquired from SCALGO Live*
- *Municipality borders in polyline and polygon format acquired from SCB and Lantmäteriet*

Table 1 illustrates the names given to various datasets in the 3.3 section.

Table 1: Explanation of names given to the datasets in the following chapters.

Generated data	Data type	Name given in following chapters
DEM depicting elevation change between year 2019 and 2023	Raster	Substracted DEM
Zone displaying the area from dune top to dune toe	Polygon	Zone 1
Zone displaying the area from dune toe to waterline	Polygon	Zone 2
Zone displaying entire beach area, from dune top to waterline	Polygon	Beach area polygon
RKT-GNSS points from years 2021-2023	Polygon	GPS point
DEM from the year 2023	Raster	DEM 2023
DEM from the year 2019	Raster	DEM 2019

Table 2 illustrates all the GPS points, their location as well as the date they were measured.

Table 2: Illustration of GPS points, their location as well as the date they were measured.

GPS-point location	Date
Falsterbo, Vellinge	2023-10-25
Falsterbo, Vellinge	2023-10-22
Falsterbo, Vellinge	No Date
Falsterbo, Vellinge	2023-10-21
Falsterbo, Vellinge	2023-10-18
Falsterbo, Vellinge	2023-10-24
Löderup, Ystad	2023-10-30
Löderup, Ystad	2023-08-28
Löderup. Ystad	2023-06-28
Löderup, Ystad	2023-05-02
Löderup. Ystad	2023-02-23
Löderup. Ystad	2023-01-19
Löderup, Ystad	2022-12-19
Löderup, Ystad	2022-11-11
Löderup, Ystad	2022-10-26
Skurup	2021-09-01
Vik, Simrishamn	2023-02-07
Kämpinge, Vellinge	2023-10-21
Åhus & Kivik, Simrishamn	2023-12-07
Knäbäckshus & Kåseberga, Ystad and Simrishamn	2023-12-18
Nybrostrand & Abbekås, Ystad	2023-12-20

3.2.2 Software

The following software was used during the analysis.

- *ArcGIS Pro Software (2.7.0, 2020 Esri Inc.)*

- *Excel (Microsoft® Excel® for Microsoft 365 MSO (Version 2304 Build 16.0.16327.20200)*
- *SCALGO Live*

3.3 Methodology

3.3.1 Coastal Monitoring Through ArcGIS

The following paragraphs under 3.3.1 describe the methodology behind the elevation change analysis done in ArcGIS. Section 3.3.1.1 describes the digitizing and image interpretation method whereas section 3.3.1.2 describes the methods of zoning and volume change analysis.

3.3.1.1 Digitizing Process

In order to conduct the analysis, polylines illustrating dune top, dune toe, and the waterline were digitized manually. The reason for manually digitizing the polylines, rather than automating the process through tools like iBluff and CliffDelinia, is to yield a higher precision, as dune tops vary in length along the coast. In addition, dunes in some areas had a low elevation, while absent in other areas. As numerous of the aforementioned tools account for bluffs and cliffs which are usually high in elevations, interpretation errors could arise.

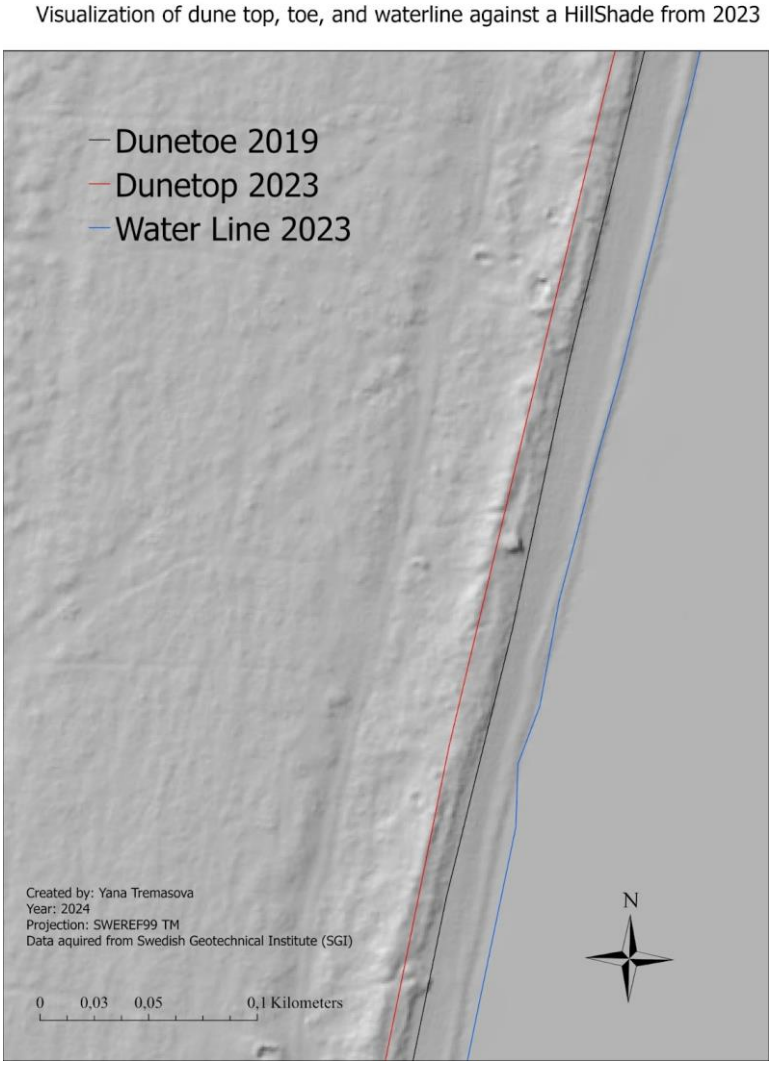

Figure 3: Illustration of dune top, toe and waterline placements over the eastern part of the study area, against a HillShade from year 2023.

When identifying dune tops and toes, several factors were considered, including slope gradients, contour lines at 0.3 m intervals, orthophotos, and HillShade derived from DEM 2019 and from DEM 2023. Furthermore, DEM depicting elevation changes between 2023 and 2019 was utilized. This DEM shows both negative changes (erosion) and positive changes (accumulation) and was acquired through the subtraction

of 2023 from 2019 DEM. Both visual (HillsShade and orthophotos) and numerical (contour lines and slope) data facilitated the accurate identification of dune crests. Numerical data also reduce the level of subjectiveness. The dune tops line was constructed from the 2023 DEM and identified based on where the slopes were leveling out, as well as the highest contour line value. To exclude the capturing of other topographical features rather than dune tops, the contour lines typically did not exceed 20 meters of height. Similarly, orthophotos were used to maintain spatial accuracy within the coastal area boundaries and to avoid encroachment into infrastructure and vegetational areas. In contrast, dune toes were based on 2019 DEM and identified at points where the slope data transitioned from steep to more level, and where contour lines corresponded to elevations of approximately 0.9 to 1.2 meters. The reason behind this was to have a margin above water level and to not capture the entire shoreline plane. Regarding both dune top and toe, notice was taken to the subtracted DEM when digitizing. This was done to ensure the capture of areas demonstrating the most significant changes in both erosion and accumulation. Lastly, waterline was digitized mainly through orthophotos and contour lines from 2023 DEM with elevation being equivalent to as low as 0,3 meters. Illustration of finalized polylines are shown in fig 3.

Various maps were made for the purpose of showing areas with extreme accumulation and erosion values. These maps were based on the subtracted DEM, which was classified into five categories ranging from negative to positive values. Based on this data, two polylines were digitized illustrating where accumulation exceeded 0.3 and 0.6 m, respectively. Additional two polylines were also digitized based on areas where erosion exceeded the same values, i.e., 30 and 0.6 m respectively.

3.3.1.2 Conducting Volume Change Analysis

Volume change assessment was conducted through zoning. First, a polygon representing the entire beach area, from dune top to waterline was created. The subtracted DEM was clipped into the beach area polygon. Since the subtracted DEM shows elevation values as floating points, it cannot generate an attribute table which is crucial for this analysis. Therefore, the subtracted DEM was multiplied by 10000, and then transformed into an integer. Consequently, an attribute table could be created.

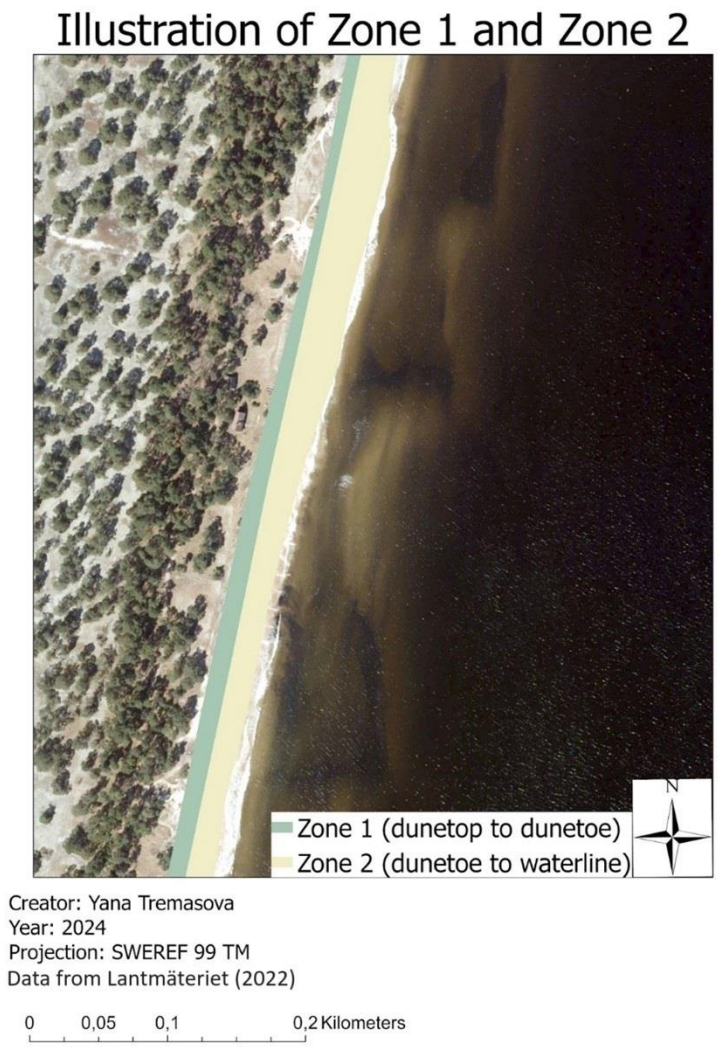

Figure 4: Illustration of zone 1 and zone 2 over the eastern side of the study area

Due to the size of the study area, it was decided to calculate the volume change in cubic meter/meter (m^3/m) for each municipality respectively. To do this, a feature illustrating municipal borders from Lantmäteriet was downloaded and harmonized into SWEREF99 TM projection. Subsequently, the generated polylines (dunetop, dunetoe, waterline) were divided to each concerning municipality. After this, they were created into two additional polygons, as seen in fig. 4: one representing Zone 2 (the area between waterline and dune toe), and another representing Zone 1 (the area between dune toe and dune top). The subtracted DEM was later further clipped into Zone 1 and Zone 2 divided by each municipality.

To obtain correct elevation values in decimals, the subtracted DEM had to be divided by 10000 and multiplied by the "count" field in the attribute table, which indicates how many pixels were assigned to each value. The reasoning for multiplying the DEM values with "count" field was to avoid getting an underestimate of the total elevation value, which potentially leads to inaccurate volume calculations or misinterpretations of the overall topography. To get the resulted value in cubic meters, the field was further multiplied by one, as the pixel size of the subtracted DEM is 1x1 meters. From this calculated output, the sum of negative and positive values was calculated, and divided individually by the total length of municipality which was

based on the waterline polyline. The result yields a volume change in m^3/m. These steps were done repetitively for each municipality.

The paragraphs above provide a simplified overview of volume change assessment. A more site-specific analysis was specifically done for small areas in Ystad and Simrishamn municipality. This analysis involved calculating volume change per square meter (area). The reasoning for this being that calculating volume change per m^2 provides a more accurate representation of the terrain's changes, as it accounts for the differing and uneven areas of the polygon rather than solely estimating volume change per specified length along a coastal stretch. For the site-specific analysis, beach area polygon was clipped into the latter municipalities individually. This polygon was later subdivided into equal areas of 1000 square meters (m^2) and clipped further into zone 1 and zone 2. Then, positive and negative values were extracted from the subtracted DEM in zone 1 and zone 2 respectively. Finally, zonal statistics was used to calculate volume change for each area within the zone 1 and 2 polygons. The results were later exported into MS Excel. Due to the output from this analysis containing a large extent of data, it would be difficult to visualize the result. Therefore, a sample of 20 polygons were chosen randomly in the east and south coast respectively. The summed elevation value for each polygon within the chosen area was later divided by 1000 in order to get the change per m^2.

As the aforementioned steps only yield a statistical result, a hotspot analysis (Getis-Ord-Gi*) was conducted for visualization purposes. A hotspot analysis creates high and low clustering values, where each cell, representing an elevation value, is compared to neighboring cells. In order for a feature to be a statistically significant “hotspot”, it must have a high value and be surrounded by other features that also have high values (ESRI, n.d.*a*). Therefore, this analysis offers a more precise depiction of erosion and accumulation locations rather than just using the subtracted DEM. The threshold for neighboring features was set to ten meters in order to generate higher precision. Moreover, this tool generates z- and p-values which tell whether the values are above (positive z-value) or below (negative z-value) the mean. Similarly, p-value indicates whether the elevation change happened due to the random chance alone (high p-value) or not (low p-value) (ESRI, n.d.*b*). This hotspot analysis was done for the entire zone 1 and 2 respectively. The output generates three classes: coldspots (erosion), hotspot (accumulation), and non-significant elevation changes. The hotspot analysis was not used in any calculation of the volume change. The reasoning for this was that this analysis does not consider all elevation changes, resulting in an underestimation of the actual elevation change. Nevertheless, it serves a valuable purpose in visualizing sediment transportation in southern and eastern coast.

3.3.2 Map Quality Assessment

As mentioned in the background section 2.3, LiDAR scanned data can generate interpretation errors due to various reasons such as cloud cover. In order to evaluate the accuracy of the DEMs

used, a map accuracy assessment was conducted. For this, ground data transect points gathered through RTK-GNSS were acquired from SGI. These point data contain elevation as well as the coordinates of where each point was taken. The dataset covers GPS points in the form of transects along the study area, taken at different dates before and after Babet. Numerous points showed negative elevation values as they crossed the waterline. To account for this, the digitized waterline was used to erase all the points that crossed it. The tool "*spatial join*" was used in order to join DEMs from 2023 and from 2019 to each transect. This tool joins the elevation values based on the spatial relationship. The joint attribute table from each transect was later exported into MS Excel, where further assessments were made.

For each transect, a scatter plot was made to illustrate a visual relationship between the observed values (transects) and the predicted values (DEMs). In addition, R^2 values, showing the statistical relationship between the dependent and independent values, were added to each scatter plot. The closer R^2 is to 1, the stronger the relationship between the dependent and independent values. Likewise, root mean square error (RMSE) was calculated for DEM 2023 and 2019 individually, in relation to each transect. The closer the value is to 0, the better the fit (Olumide, 2023). Unlike other ways to summarize data, such as through the mean, standard deviation, and maximum error, RMSE is used to evaluate DEMs accuracy and precision in relation to the GPS points (Polidori & El Hage, 2020; Alganci, et al., 2018).

4 Results

4.1 Volume change Assessment

Fig. 5 is displayed as a visualization map, showing eroded areas by 0.3 m and higher above the sea level. The zoomed in locations are examples of areas most affected by erosion. It can be seen that the majority of the study area experienced a negative change in elevation, with minor gaps in the southeast, southwest, and northeast regions. The example areas in Simrishamn (1.) and Vellinge (2.) municipalities have significant changes throughout the majority of the coastal area in the zoomed in locations whereas Ystad (3.) has minor changes. Moreover, there seems to be an even recurrence between erosion exceeding 0.3 m and erosion exceeding 0.6 m in all three zoomed in example areas.

Figure 5: Map of Scania displaying areas where sediment eroded by > 0.3 m (red line) and > 0.6 m (black line), depicting three example areas of Simrishamn, Vellinge, and Ystad municipalities as zoomed in illustrations.

Similarly to fig. 5, fig 6 is displayed as a visualization map. It can be seen that positive elevation changes cover the majority of the study area as well. However, Bromölla and Sölvesborg indicate little to no accumulation above 0.3 m. It can also be seen on the zoomed in aera of Simrishamn (1), Vellinge (2.), and Ystad (3.) municipalities that there is a variation between accumulation exceedances. It can be observed that accumulation of 0.3 m is more recurring than that of 0.6 m all the zoomed in areas in the map. Furthermore, Haväng and Falsterbo seem to be consistent with erosion and accumulation amounts in both fig 5 and 6, whereas Nybrostrand varies. Nybrostrand experiences more accumulation than erosion which can be seen in fig. 6.

Figure 6: Map of Scania displaying areas where sediment has accumulated by > 0.3 m (red line) and > 0.6 m (black line), depicting three example areas of Simrishamn, Vellinge, and Ystad municipalities as zoomed in illustrations.

Table 3 shows volume change in m^3/m within different municipalities in zone 1. Overall, Ystad has the highest accumulation and erosion values of -4.33 m^3/m in zone 1. In contrast, Bromölla has the lowest accumulation and erosion values of -0.01 m^3/m in zone 1.

Values for erosion and accumulation within municipalities alter significantly, although it can be observed that all municipalities have higher values of erosion than accumulation, making the total volume change negative.

Table 3: Volume change in cubic meters per meters (m^3/m) for all 8 municipalities in zone 1 situated within the study area.

Municipality (zone 1)	Accumulation (m3/m)	Erosion (m3/m)	Total (m3/m)
Vellinge	1.95	-3.94	-1.99
Trelleborg	0.77	-3.16	-2.39
Skurup	0.56	-4.52	-3.96
Ystad	2.66	-6.99	-4.33
Simrishamn	1.71	-2.45	-0.74
Kristianstad	0.43	-2.02	-1.59
Bromölla	0.08	-0.09	-0.01
Sölvesborg	0.22	-0.73	-0.51

Table 4 shows volume change in m^3/m within different municipalities in zone 2. Similar to table 2, Ystad exhibits the highest values in both accumulation and erosion values. However, due to the similarity between erosion and accumulation values, these balance each other out. This results in Ystad being one of the municipalities with the least overall change of -0.36 m^3/m in zone 2. In contrast, Simrishamn has the highest positive total change out of all the municipalities of 1.53 m^3/m and Kristianstad has the highest negative total change of -1.14 m^3/m. Additionally, it can be observed that Sölvesborg municipality displays the lowest changes in accumulation and erosion values as well as lowest overall changes of -0.16 m^3/m.

Unlike zone 1, the overall change between the municipalities varies between accumulation and erosion. Ystad, Kristianstad, Bromölla, and Sölvesborg experience loss of sediment while Simrishamn, Skurup, Trelleborg, and Vellinge experienced accumulation.

Table 4: Volume change in cubic meters per meter (m^3/m) for all 8 municipalities in zone 2 situated within the study area.

Municipality (zone 2)	Accumulation (m3/m)	Erosion (m3/m)	Total (m3/m)
Vellinge	1.13	-0.75	0.38
Trelleborg	1.22	-0.95	0.28
Skurup	1.66	-0.47	1.19
Ystad	3.14	-3.50	-0.36
Simrishamn	3.00	-1.47	1.53
Kristianstad	1.33	-2.48	-1.14
Bromölla	0.10	-0.71	-0.60
Sölvesborg	0.08	-0.24	-0.16

Fig. 7 illustrates the area of Rörum where the site-specific analysis was conducted. It can be seen that the area near the shoreline plain exhibits higher accumulation than area near the dunes, which experiences less accumulation and less significant change overall.

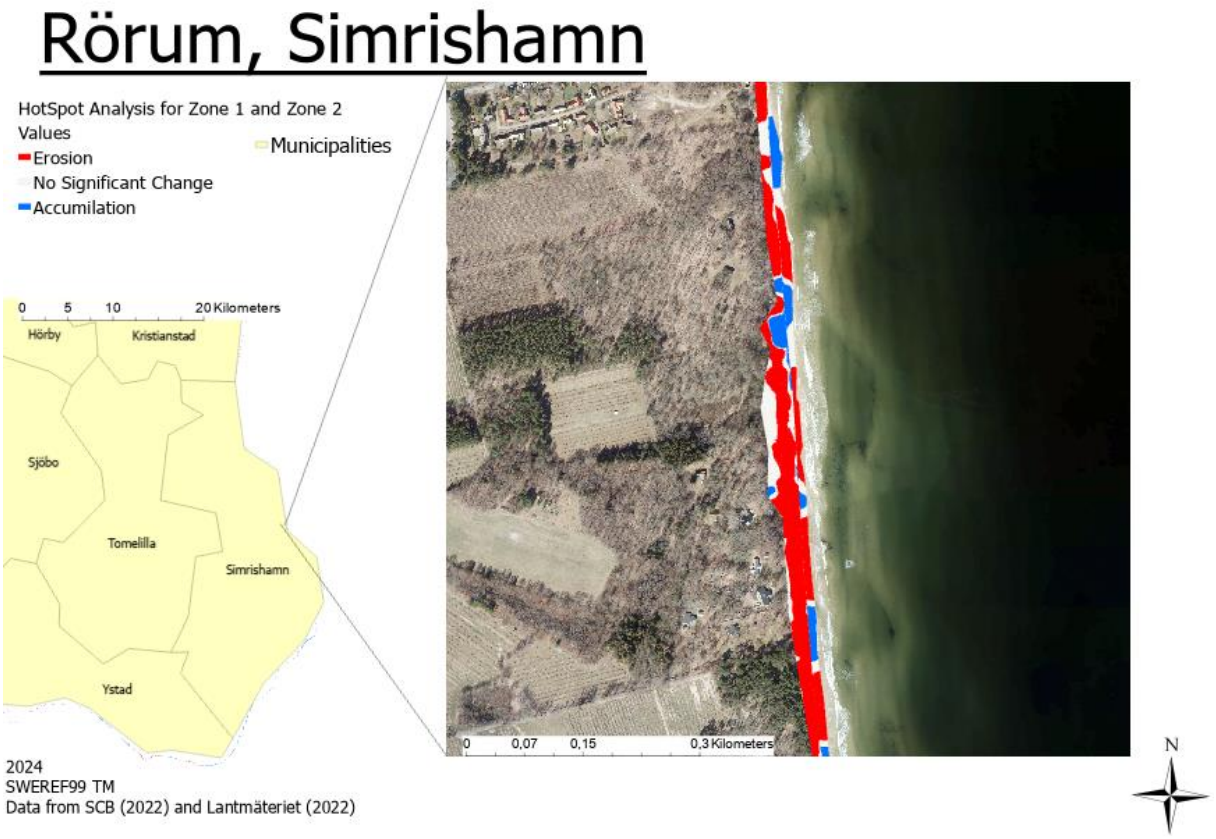

Figure 7: HotSpot analysis conducted on the area of Rörum, Simrishamn, showcasing areas of significant erosion (red) and accumulation (blue) as well as areas with no-significant changes (light gray).

Fig. 8b shows the volume change assessment in the unit of m^3/m^2 in zone 2 in Rörum, Simrishamn. It can be seen that the accumulation is generally higher than erosion, which mostly stays constant and near zero. In contrast, fig. 8a, which shows zone 1 in the same area, has a more equal alternation between the positive and negative values. The highest values in both zones are similar, showcasing the highest erosion value to be m^3/m^2 and highest accumulation value to be 0.27 m^3/m^2. Likewise, the lowest value in both zones is equal to 0 m^3/m^2.

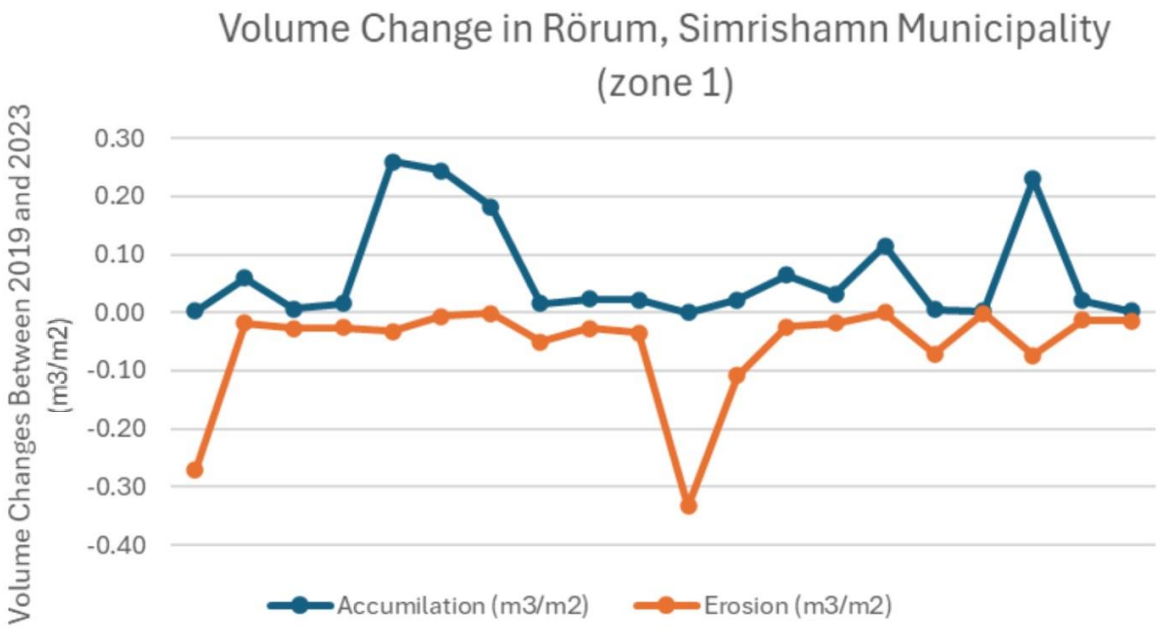

Figure 8a: Displays a site-specific volume change assessment in zone 1 in the area of Rörum, Simrishamn Municipality, where Y-axis represents the volume change in m³/m².

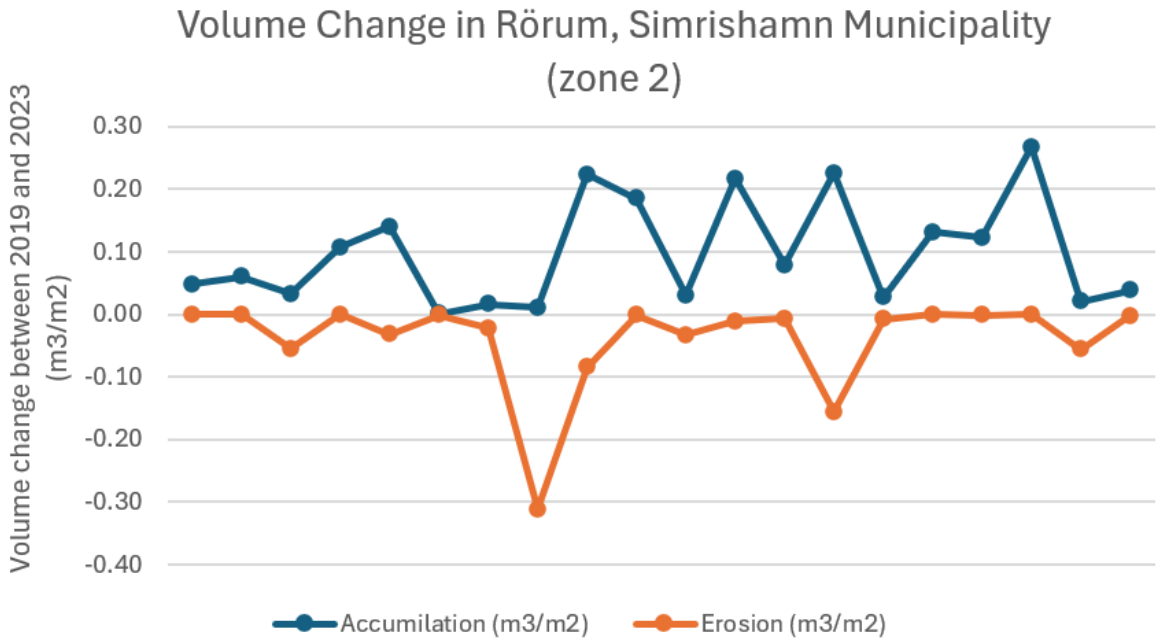

Figure 8b: displays a site-specific volume change assessment in zone 2 in the area of Rörum, Simrishamn Municipality, where Y-axis represents the volume change in m³/m².

Fig. 9 shows the location of Anton Fiskares väg, Ystad, where site-specific volume change analysis was conducted. It can be seen that zone 1 and 2 exhibits similar accumulation and erosion amounts. However, when comparing this to fig. 10a and 10b, zone 1 depicts higher alternation between erosion values than zone 2.

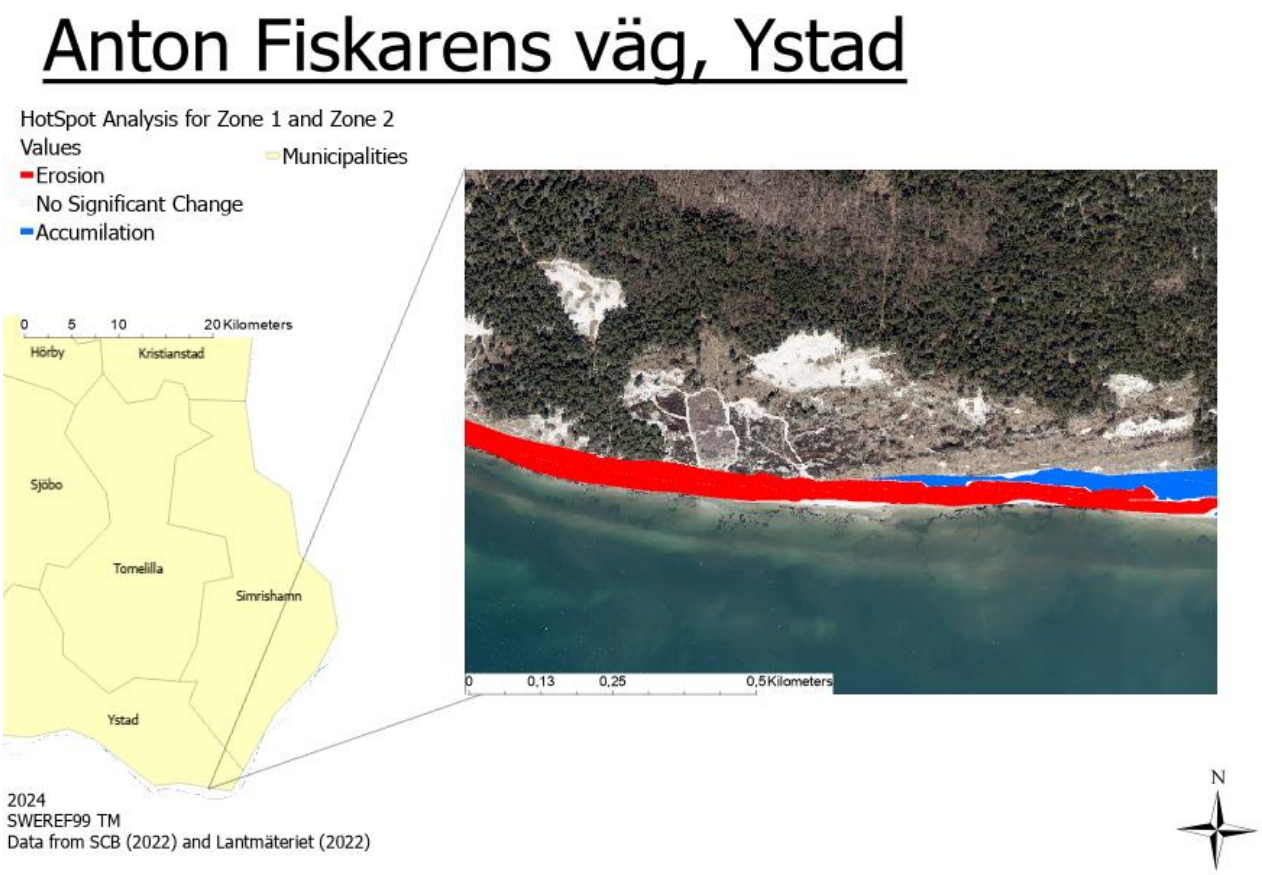

Figure 9: HotSpot analysis conducted in the area of Anton Fiskares väg, Ystad, showcasing areas of significant erosion (red) and accumulation (blue) as well as areas with no-significant changes (light gray).

Fig. 10a and 10b showcases a site-specific volume change analysis in cubic meter per square meter in zone 1 and 2 conducted in Anton Fiskares väg, Ystad. Fig. 10a illustrates higher alternation in erosion than accumulation values, which are more constant and near 0. The highest accumulation value is 0.35 m^3/m^2 whereas the lowest is 0 m^3/m^2. The highest erosion value is near -0.60 m^3/m^2 whereas the lowest is 0 m^3/m^2.

Fig. 10b on the other hand depicts a higher volume change throughout the majority of the area. The highest accumulation value is 0.32 m^3/m^2 whereas the lowest is 0 m^3/m^2. The highest erosion value is -2.2 m^3/m^2 and the lowest is 0 m^3/m^2.

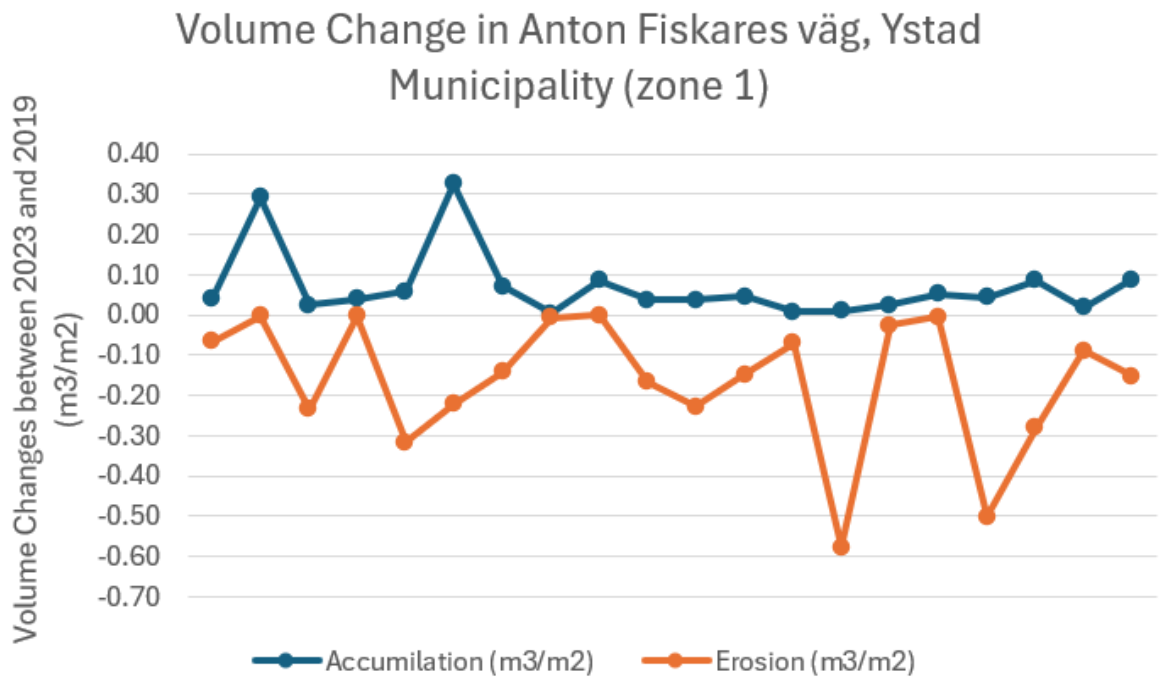

Figure 10a: Displays a site-specific volume change assessment in zone 1 in the area of Anton Fiskares väg, Ystad Municipality, where Y-axis represents the volume change in m³/m².

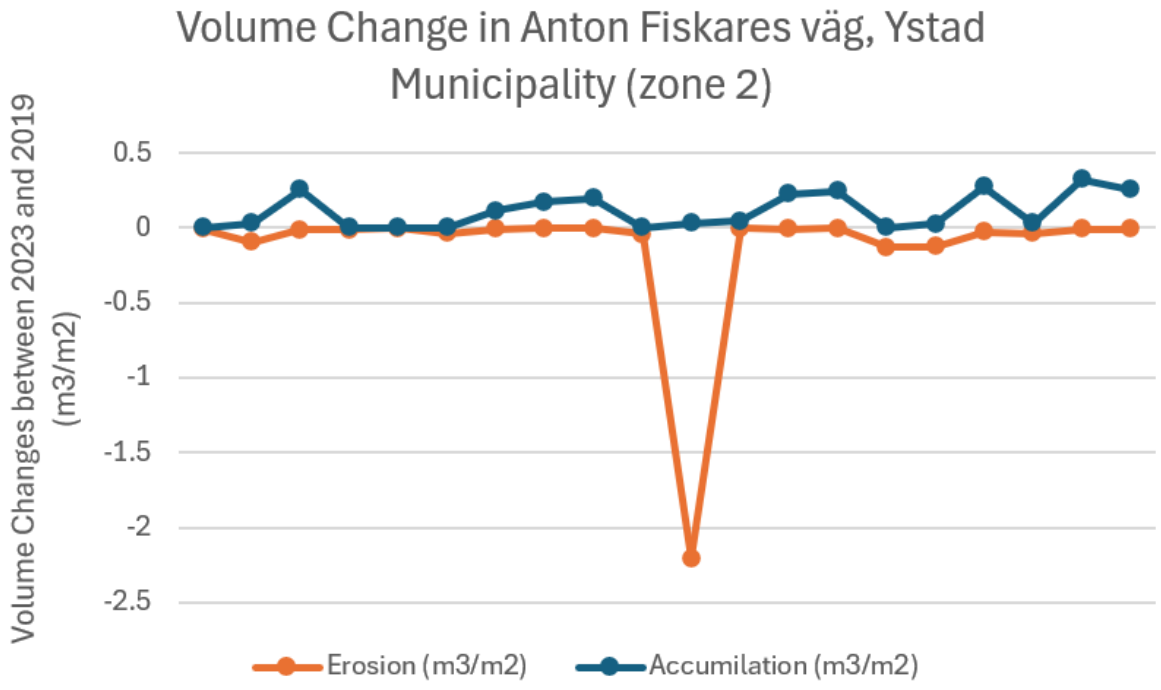

Figure 10b: Displays a site-specific volume change assessment in zone 2 in the area of Anton Fiskares väg, Ystad Municipality, where Y-axis represents a volume change in m³/m².

4.2 Map Quality Assessment

It is important to note that not all scatterplots will be displayed under this chapter. For more clarification, refer to chapter 8.2.

It can be seen in fig. 11 a and b that DEMs from both years in Falsterbo, Vellinge depict a good linear relationship, with R^2 values being relatively close to 1. The DEM from 2023 has a slightly higher R^2 value than the DEM from 2019, which is more scattered with outliers showing between 2 and 4 meters. Moreover, both fig. 11a and b appear to exhibit a similar pattern: they are initially linear, then gradually become more scattered before returning to the linear trend.

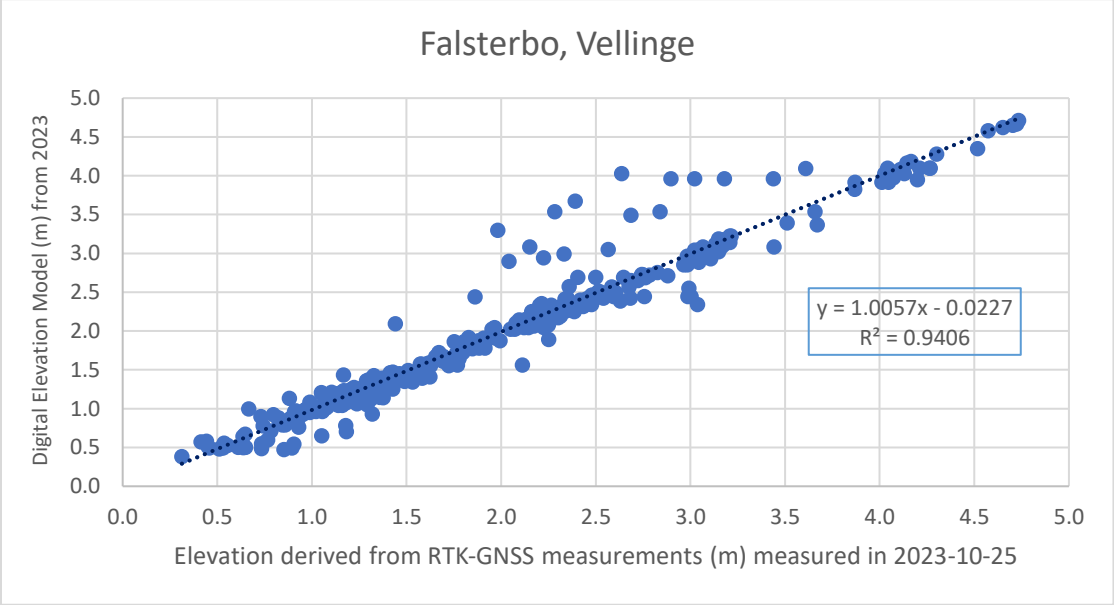

Figure 11a: Scatter Plot depicting the relationship between predicted values (DEM from 2023) against observed values (RTK-GNSS) in Falsterbo, Vellinge. The linear dotted line represents the best fitted straight line between the predicted and observed values. Ground data measured in 2023-10-25.

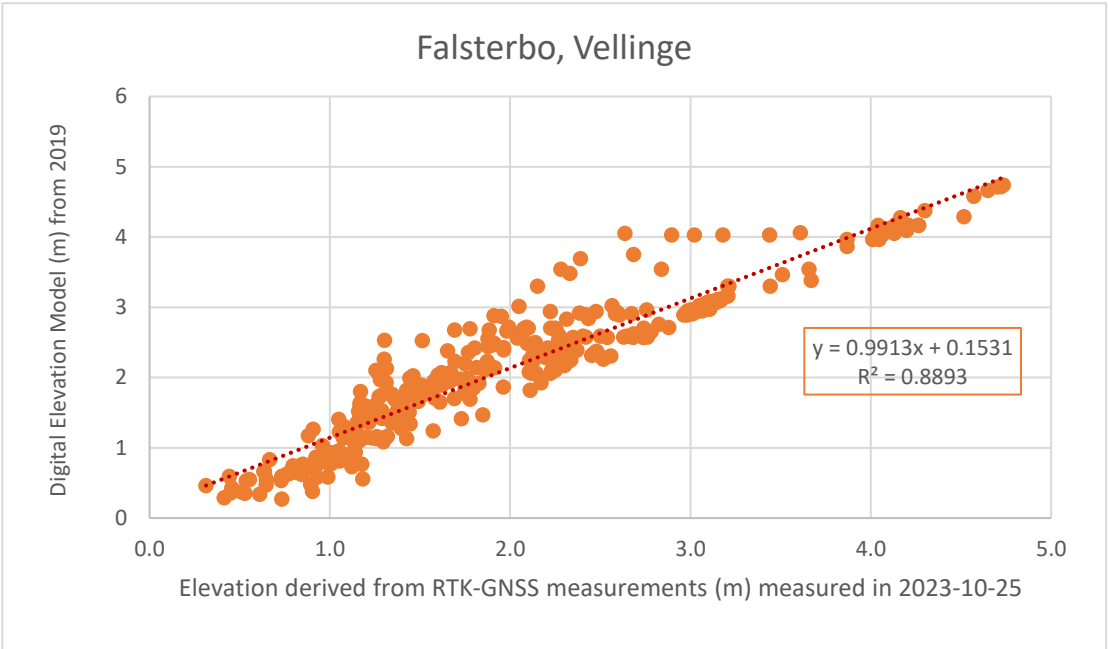

Figure 11b: Scatter Plot depicting the relationship between predicted values (DEM from 2019) against observed values (RTK-GNSS) in Falsterbo, Vellinge. The linear dotted line represents the best fitted straight line between the predicted and observed values. Ground data measured in 2023-10-25.

Fig. 12 a and b depict the relationship between predicted and observed values in Vik, Simrishamn. The scatter plot shows a good linear regression for both DEMs with R^2 values being 0.94 and 0.97. DEM from 2023 has a slightly higher R^2 value than DEM from 2019. It can be seen in fig. 12b that it is more scattered between 10 to 16 meters than fig. 12a.

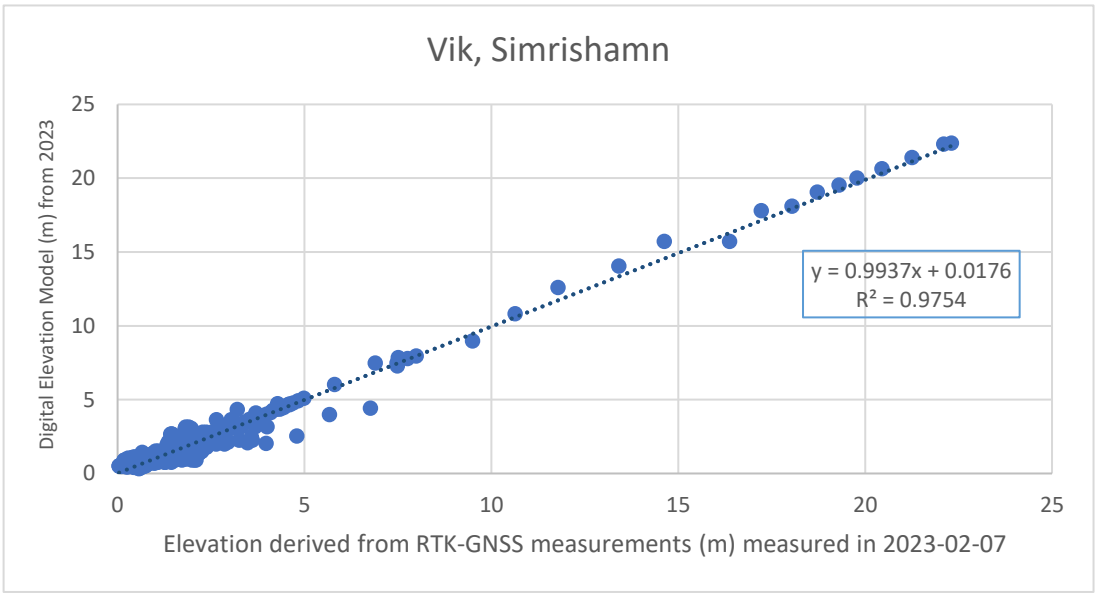

Figure 12a: Scatter Plot depicting the relationship between predicted values (DEM from 2023) against observed values (RTK-GNSS) in Vik, Simrishamn. The linear dotted line represents the best fitted straight line between the predicted and observed values. Ground data measured in 2023-02-07.

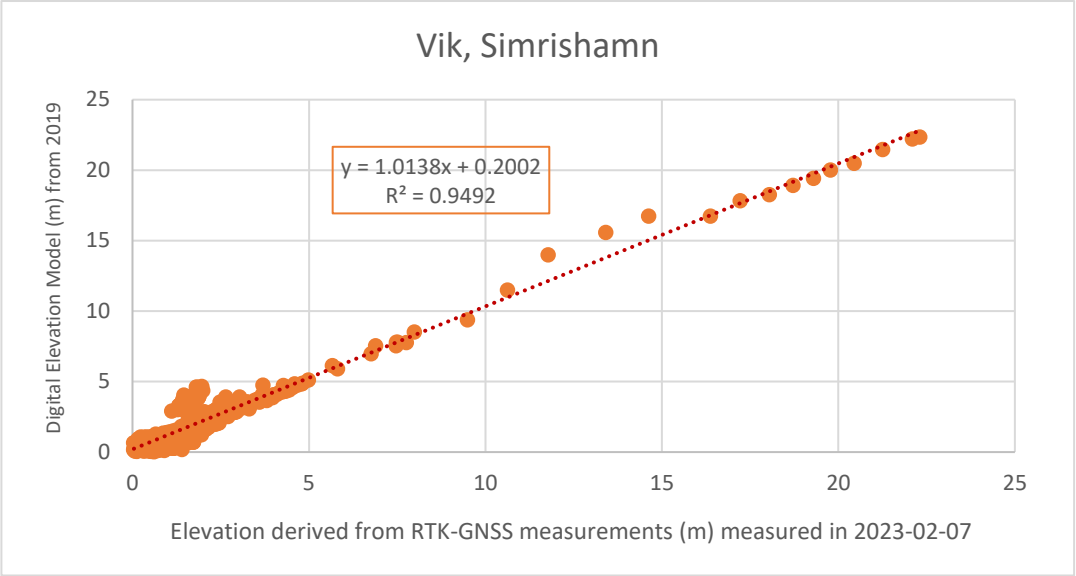

Figure 12b: Scatter Plot depicting the relationship between predicted values (DEM from 2019) against observed values (RTK-GNSS) in Vik, Simrishamn. The linear dotted line represents the best fitted straight line between the predicted and observed values. Ground data measured in 2023-02-07.

Fig. 13 a and b depict the relationship between predicted and observed data against GPS points in Kämpinge, Vellinge. It shows that both DEMs have a low linear relationship with R^2 being as low as 0.47 for DEM 2019 and 0.26 for DEM 2023. DEM 2019 has a higher R^2 value and is less scattered than DEM 2023. Although, it can be seen that both fig. 13 a and b have as big outliers as 1 meter from the trendline. These outliers are, however, situated in different places on the figures.

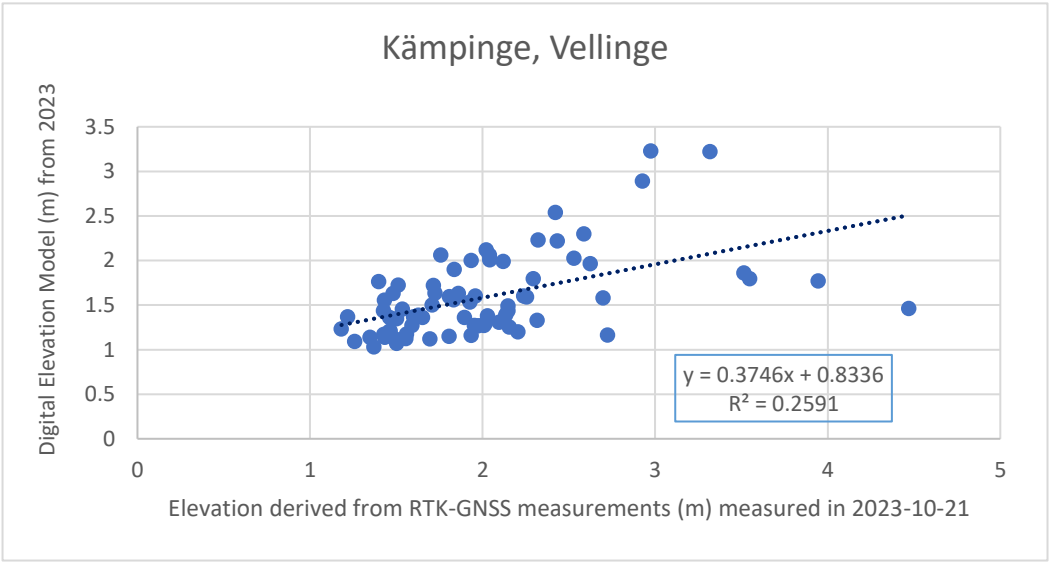

Figure 13a: Scatter Plot depicting the relationship between predicted values (DEM from 2023) against observed values (RTK-GNSS) in Kämpinge, Vellinge. The linear dotted line represents the best fitted straight line between the predicted and observed values. Ground data measured in 2023-10-21.

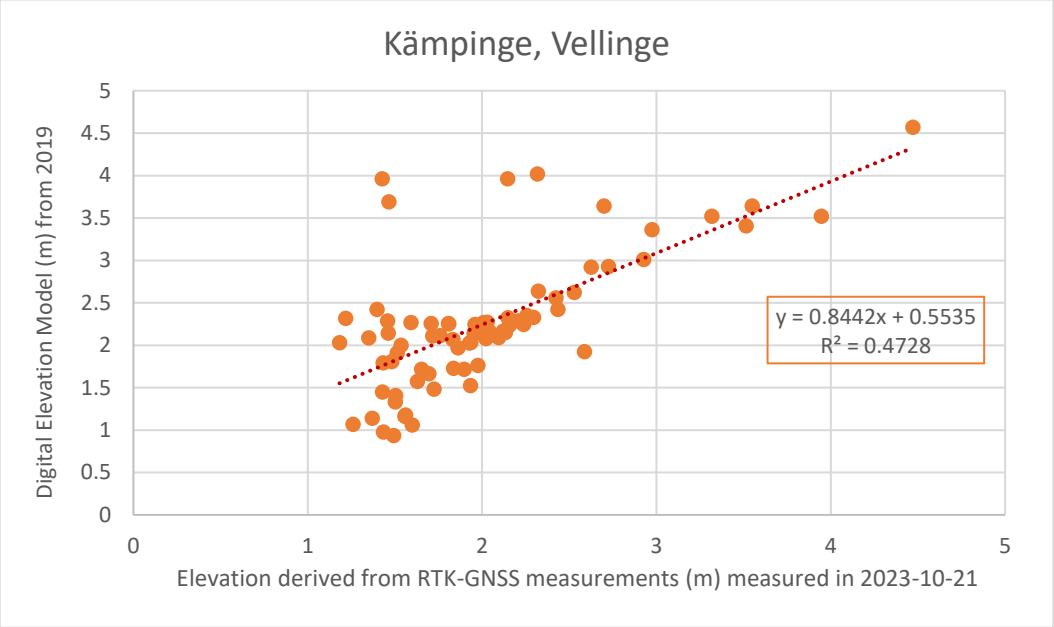

Figure 13b: Scatter Plot depicting the relationship between predicted values (DEM from 2019) against observed values (RTK-GNSS) in Kämpinge, Vellinge. The linear dotted line represents the best fitted straight line between the predicted and observed values. Ground data measured in 2023-10-21.

Fig. 14 a and b depicts the relationship between predicted and observed values in Löderup, Ystad. Here, the scatter plot shows higher R^2 values than fig. 13a-b, but lower values than fig. 11a-b and 12a-b. R^2 in DEM 2019 is higher than in DEM 2023. When comparing this to fig.14a, it can be seen that the points are significantly more dispersed throughout the whole graph showcasing a more altering elevation in the area.

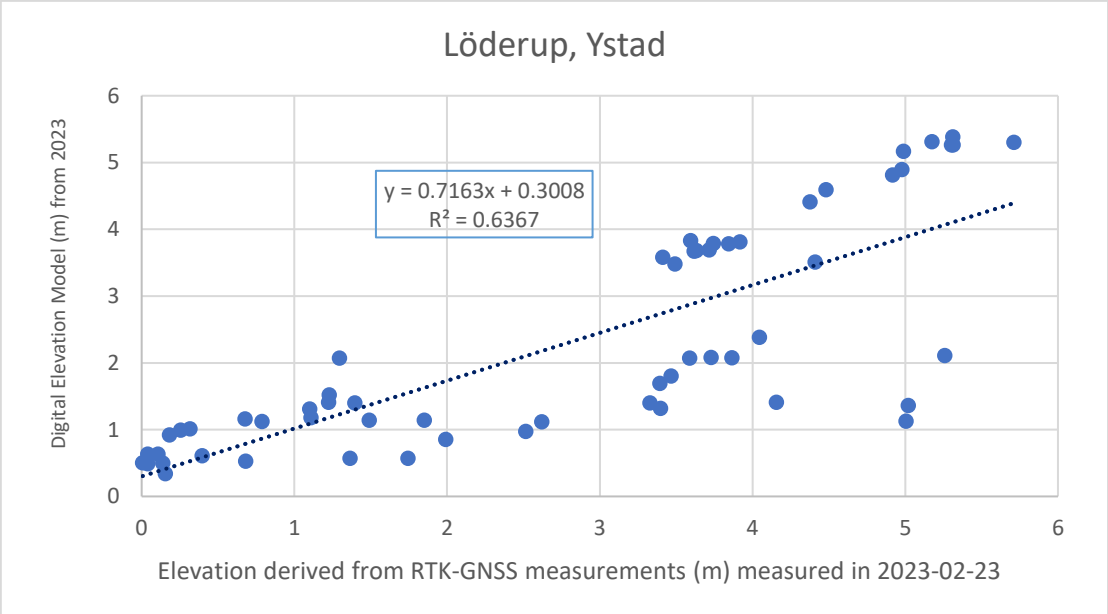

Figure 14a: Scatter Plot depicting the relationship between predicted values (DEM from 2023) against observed values (RTK-GNSS) in Löderup, Ystad. The linear dotted line represents the best fitted straight line between the predicted and observed values. Ground data measured in 2023-02-23.

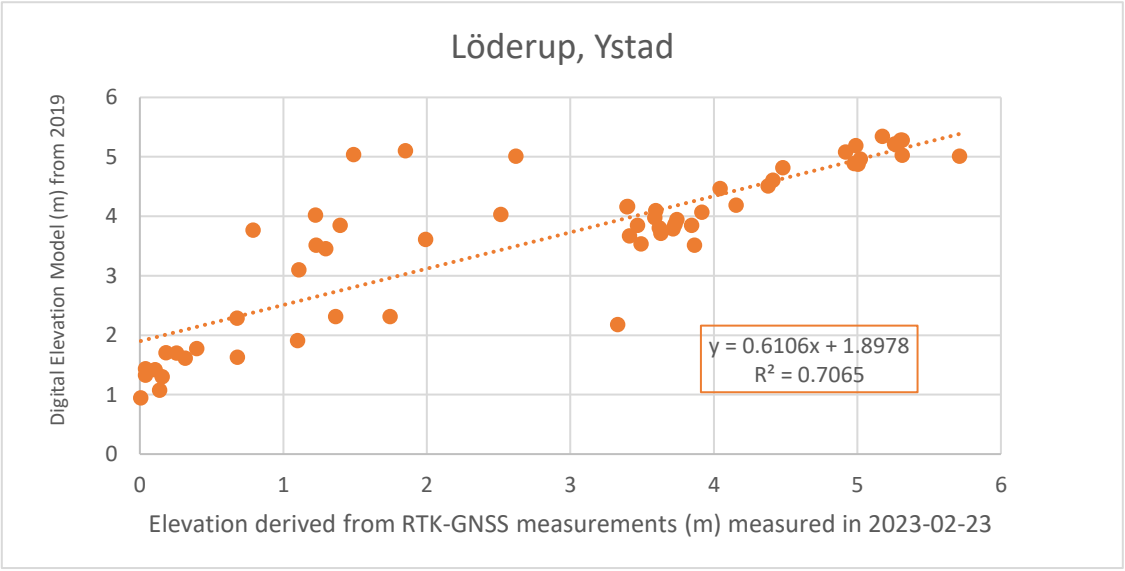

Figure 14b: Scatter Plot depicting the relationship between predicted values (DEM from 2019) against observed values (RTK-GNSS) in Löderup, Ystad. The linear dotted line represents the best fitted straight line between the predicted and observed values. Ground data measured in 2023-02-23.

Table 5 indicates that DEM from 2023 in Kämpinge has the highest RMSE value (0.70), while Åhus has the lowest (0.26). This trend can also be seen in fig. 15, showing that Kämpinge has more scattered values, and hence a lower relationship between observed and predicted values.

In addition, it can also be seen that Kämpinge has the lowest R^2 value of 0.26, which further confirms the weak relationship between the predicted and observed values. In contrast it can be seen that Åhus has one of the highest R^2 values which confirms the strong relationship between the predicted and observed values.

In comparison, the DEM from 2019 demonstrates that Vik has the highest RMSE value (0.76) and as well as the highest R^2 value (0.95) indicating that there is a strong correlation but high difference between the DEM and GPS points. On the other hand, Skurup has the lowest RMSE (0.32), but a significantly high R^2 value (0.82). In contrary, Kämpinge has the lowest R^2 (0.47) value and a significantly high RMSE value (0.62) signifying weak both relationship and indifference between the DEM and GPS points.

Table 5: Illustration of root mean square error (RMSE) and R^2 values for each GPS point location against DEM from 2023 and 2019

GPS points Location, Date (YYMMDD)	Skurup, 210901	Vik, 230207	Kämpinge, 231021	Åhus, Kivik, 231207	Knäbäckshus, Kåseberga, 231218	Nybro, Abbekås, 231220
RMSE	0.51	0.48	0.70	0.26	0.44	0.35
R^2	0.63	0.98	0.26	0.95	0.91	0.92
Digital Elevation Model (Year)	**2023**	**2023**	**2023**	**2023**	**2023**	**2023**
RMSE	0.32	0.76	0.62	0.57	0.68	0.63
R^2	0.82	0.95	0.47	0.83	0.77	0.81
Digital Elevation Model (Year)	**2019**	**2019**	**2019**	**2019**	**2019**	**2019**

In comparison to table 5, table 6 indicates overall higher RMSE values, showcasing a higher difference between observed and predicted values in Löderup, Ystad. The highest RMSE value for DEM 2023 is depicted on the GPS points taken on 19th of December 2022, whereas the lowest is on the 30th of October 2023. The highest R^2 value is shown on the GPS points from 30th of October 2023, and the lowest is shown on GPS points from 28th of august 2023. This means that the correlation between the predicted and observed values is strongest and the differences are lowest on the GPS points from 30th of October 2023.

The highest RMSE for DEM 2019 is shown on the 30th of October 2023, whereas the lowest value is shown on the 11th of November 2022. Similarly, the highest R^2 value is shown on the 11th of November 2022 as well as on the 26th of October 2022 and the lowest R^2 value is shown on the 30th of October 2023. Overall, this shows that GPS points measured on 30th of October 2023 show the lowest correlation and the highest difference between predicted and observed values against DEM 2019. Whereas GPS points measured on the 26th of October 2022 have the strongest relationship and the lowest difference between the predicted and observed values.

Table 6: Illustration of root mean square error (RMSE) and R^2 values for each GPS point location against DEM from 2023 and 2019 in Löderup, Ystad

GPS points in Löderup, Date (YYYY-MM-DD)	2023-10-30	2023-08-28	2023-06-28	2023-05-02	2023-02-23	2023-01-19	2022-12-19	2022-11-11	2022-10-26
RMSE	0.58	1.32	1.32	1.27	1.21	1.43	1.38	1.42	1.36
R2	0.88	0.52	0.57	0.59	0.64	0.53	0.67	0.55	0.54
Digital Elevation Model (Year)	**2023**	**2023**	**2023**	**2023**	**2023**	**2023**	**2023**	**2023**	**2023**
RMSE	1.83	1.32	1.18	1.22	1.29	1.06	1.15	0.83	0.96
R^2	0.39	0.65	0.69	0.62	0.71	0.69	0.65	0.81	0.81
Digital Elevation Model (Year)	**2019**	**2019**	**2019**	**2019**	**2019**	**2019**	**2019**	**2019**	**2019**

Table 7 indicates a low overall RMSE values for both DEM 2023 and 2019 while R^2 values are higher for DEM 2023 than DEM 2019 in Falsterbo, Vellinge. It can be seen that for DEM 2023, GPS points measured on 18th October 2023 have the highest RMSE value while 24th October 2023 has the lowest. R^2 value is highest on the 24th of October 2023 and lowest on the 18th of October 2023. Overall, GPS points measured on the 24th of October 2023 have the strongest correlation and the lowest differences between the observed and predicted points whereas 18th of October 2023 have the lowest correlation and highest difference between the points.

For DEM in 2019, the highest RMSE value is shown on the 21st of October 2023 whereas the lowest RMSE value is shown on the 25th of October 2023. Similarly, the highest R^2 value is also demonstrated on 25th October 2023, while the lowest is shown on the 21st of October 2023. This means that 21st of October exhibits weak relationship and high indifference between the values whereas 25th October exhibits strong relationship and more similarity between the DEM and GPS points.

Table 7: Illustration of root mean square error (RMSE) and R^2 values for each GPS point location against DEM from 2023 and 2019 in Falsterbo, Vellinge

GPS points in Falsterbo, Date (YYYY-MM-DD)	2023-10-25	2023-10-22	N.D	2023-10-21	2023-10-18	2023-10-24
RMSE	0.24	0.30	0.27	0.58	0.85	0.22
R^2	0.94	0.91	0.92	0.90	0.71	0.98
Digital Elevation Model (Year)	**2023**	**2023**	**2023**	**2023**	**2023**	**2023**
RMSE	0.36	0.66	0.54	1.71	0.74	0.66
R^2	0.89	0.73	0.79	0.40	0.77	0.86
Digital Elevation Model (Year)	**2019**	**2019**	**2019**	**2019**	**2019**	**2019**

5 Discussion

5.1 Discussion of The Results

5.1.1 Discussing Volume Change Assessment

Overall, it can be seen from figures 5 and 6 that the majority of the coastal area is affected by either accumulation or erosion values above 0.3 m. The most significant changes can be seen in the east coast area. The observation is further supported by table 4, showing that Simrishamn and Kristianstad municipalities have one of the highest volume changes per meter. Notably, there are several other municipalities experiencing noteworthy positive and negative changes including Ystad, Skurup, Trelleborg and Vellinge. As can be seen in SGU's map in fig. 2, the majority of Scania's coastal area is in condition conducive to erosion. This is especially seen in municipalities such as Vellinge, Ystad, Simrishamn, and Kristianstad which have certain areas very susceptible to sediment displacement. When comparing the results from table 3 and 4 to the first statement in the hypothesis, it is safe to say that Ystad and Simrishamn are two of the most affected municipalities, showcasing one of the highest total volume changes. It was observed from the orthophotos that the coast in the aforementioned municipalities consist mainly of loose sediments such as sand, which is mainly situated in the environment without any barriers such as larger rocks and pebbles. If there are no bigger barriers present and the threshold shear stress of the sediment is exerted, there is a higher opportunity for the sediment displacement to occur as mentioned in the background. In contrast, Bromölla and Sölvesborg exhibited the least significant change, as shown in tables 3 and 4. According to the orthophotos, Bromölla and Sölvesborg have a coastal area consisting of vegetation, bigger rocks, and pebbles rather than bare sand. Due to the increased presence of barriers and vegetation, which slows down the erosion process, it can be seen that these municipalities experience lower amounts of elevation change per meter. Another factor could be the reduced presence of sedimentary particles which naturally contributes to lower rates of sediment displacement. As depicted in the orthophoto in fig. 15, the majority of Bromölla and Sölvesborg does not have a coastal area with a beach. Instead, the coastal area is predominantly characterized by vegetation mixed with rocks and soil that leads out into the water. When comparing Bromölla and Sölvesborg to SGU's map in Fig. 2, it is also evident that these areas are not classified as having a coastline prone to erosion.

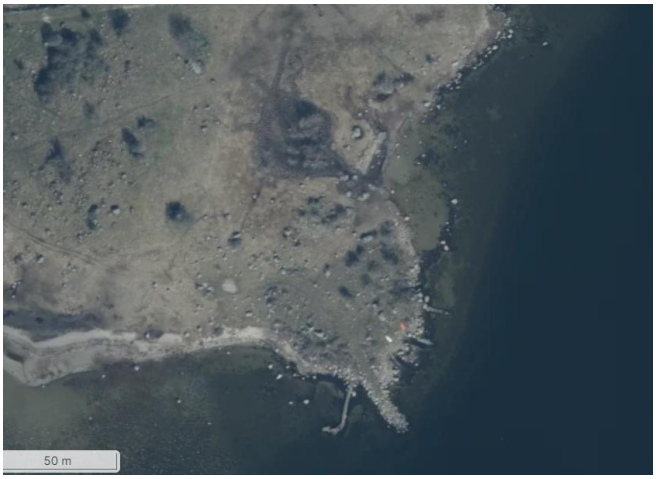

Figure 15: Illustration of the coastal area of Östersjövägen, Bromölla municipality. Data acquired from SCALGO live, 2022, downloaded from Lantmäteriet.

Additional factors that can contribute to increased accumulation and erosion values within the study area are human influence, other extreme weather events, wind patterns, or washed-up vegetation such as seaweed. As written in the background, expansion of human activity and urban settlements can lead to weakening of dunes, promoting an increased risk of erosion. Further, mitigation strategies such as beach nourishments or washed-up seaweed can

lead to morphological changes and sediment displacement. For these reasons, even though Babet was the biggest storm event between 2019 and 2023 and may have caused the majority of sediment transportation, it is impossible to attribute every change solely to the storm, introducing significant uncertainty into this study. Urban areas near the coast experience more notable erosion and accumulation compared to areas near natural environments, as depicted in appendix 1-6. The significant erosion and accumulation in urban areas supports the second hypothesis. However, this hypothesis cannot be fully confirmed, primarily because the maps in the appendix and chapter 4.1 do not provide a complete visualization of all urban areas.

Upon further comparison between table 3 and 4, it is clearly seen that zone 1 exhibits sediment loss for all the municipalities, whereas zone 2 exhibits a mixture of sediment loss and gain. This variation can be attributed to the differing environmental characteristics of these zones. Naturally, the dunes in zone 1 generally contain higher amounts of sand and sediments that can be eroded than the plain shoreline in zone 2. Referring back to the background, the sediments susceptibility of erosion depends on its placement. Erosion is more prone in areas containing steeper hillslopes. This explanation aligns with the observation that the dunes in zone 1, being tilted, show higher total erosion values in table 1. Conversely, the shoreline plane in zone 2 is more affected by factors such as barriers, tides, and wave action. Subsequently, if the presence of barriers is low, waves can either accumulate sediment or displace it elsewhere. As the majority of the study area contains postglacial sand, which is a denser particle, the majority of the sediment is being transported as bedload. As mentioned in the background, sediment transported through bedload does not travel long distances and does therefore not affect zone 1. Naturally, dominance of erosion and accumulation varies more among the municipalities in table 4. Nevertheless, it is worth noting that volume change assessment per municipal borders is a very holistic approach. Although it is a less time-consuming method, it does not go into detail in showing the location of areas experiencing significant elevation changes. Hence, it is difficult to draw conclusions on exactly where Babet caused these significant changes.

When comparing this method to a site-specific analysis as depicted in fig. 7-9, it is noticeable that erosion and accumulation occur simultaneously within the same area/zone, which is also evident in tables 3-4. This simultaneous alternation between erosion and accumulation within the same zone confirms the third statement in the hypothesis. This pattern is clearly seen for each municipality to varying degrees, as well as in the site-specific analysis fig. 7-8. On the other hand, the site-specific analysis, being applicable on a smaller scale, allows for more accurate conclusions about the causes of erosion and accumulation in specific areas. Coastal areas such as Rörum and Knäbäckshusen in Simrishamn have been hit by Babet, resulting in tree fall and major parts of the beach being washed away (Simrishamn Kommun, 2024*b*). This change can also be seen in fig. 8a and 8b, where both zone 1 and zone 2 experience varying accumulation and erosion values. Both fig. 8a and 8b show that accumulation values are more fluctuating than erosion whereas erosion has higher values than accumulation. When

combining this with fig. 7, it is seen that erosion is more persistent in both zones 1 and 2, with certain areas experiencing significant accumulation. In these blue areas, the accumulation can be attributed to the fallen trees in the area, creating barriers and slowing down erosion and increasing accumulation. Sediment supply as a result of increased runoff and wave patterns is an additional factor that can increase accumulation, especially near the shoreline plain (zone 2). As mentioned before, another factor influencing the change could be human influence. Due to Rörum being a popular beach destination, it may have led to land degradation over time. A mixture of this, the fallen trees, wind, wave intensity, and damage of the dune slope, can lead to these changes. In comparison with this, it can be noted in fig. 10a and 10b that Anton Fiskares väg experiences a bigger alternation in erosion values in zone 1, which stays nearly constant in zone 2. In addition, when comparing this to fig. 9, it can be seen that both zones 1 and 2 experience a major amount of sediment loss throughout the area. Anton Fiskares väg is situated near Hagestad which is a nature reserve and a popular tourism area, which can, similarly to Rörum, be another cause for extensive erosion. It is also seen in the orthophoto fig. 9 that Anton Fiskares väg features a mix of vegetation and open spaces allowing for more erosion to occur.

Alternatively, due to Anton Fiskares väg and Rörum being situated on the south and east coast respectively, factors such as sediment composition, differences in vegetation and wind patterns vary between the areas. This can explain the difference in volume changes between these areas. For example, if the wind is blowing towards the east, the same erosive sediment could have led to accumulation elsewhere. This is significantly seen in fig. 9, where there seems to be a substantial amount of erosion throughout the majority of the area, and accumulation in the eastern part possibly showcasing that there was a strong wind towards the east, signifying a possible relation to the storm Babet.

Upon comparing the current method with the latterly mentioned study done by Doyle & Woodroffe (2018), there seems to be similarities in the context of dune identification. Doyle & Woodroffe also combined ground measurements data (RTK-GNSS points) with LiDAR data in order to identify foredunes. However, the LiDAR data was acquired in a different way, and provided a more accurate representation, eliminating errors such as environmental factors. In addition, Doyle & Woodroffe also put higher emphasis on RTK-GPS transects when identifying dunes, allowing for a more representative identification. Further, the latter study created a TIN surface and preformed a more automated method for dune identification, combining diverse tools and scripts in ArcGIS. Determining the superiority of one method over the other for this specific study is challenging. While the methodology employed in this study was tailored to the objectives set by SGI, Doyle & Woodroffe's semi-automated approach offers potential advantages in terms of efficiency and standardization. However, it is still important to note the suitability of each method depends on factors such as the study objectives, available resources, and the desired level of precision.

5.1.2 Assessment of Availability of Data and Its Outcome

Despite centimeter-scale variations between DEM and RTK-GPS data points, the precision of the DEMs vary depending on the location and date. For example, it could be seen in fig. 11a and b that Falsterbo, Vellinge have R^2 values close to 1 for both DEM from 2023 and 2019. Whereas Fig. 13a and b depict the area of Kämpinge, Vellinge has R^2 values closer to 0 for both DEMs. This variation between uncertainties further highlights the difficulty to attribute every change to Babet. For example, the scattering and outliers in fig. 13a and b can be explained by poor RTK-GPS measurements or environmental conditions like shadows, slopes, or cloudy conditions leading to precision errors in LiDAR data.

When comparing the dates of the RTK-GPS and DEM points, the closer the date of a DEM is to GPS data points, the higher the accuracy tends to be for both RMSE and R^2 values. An example of this is seen in table 5, where DEM from the year 2023 shows significantly better relationships than DEM from 2019 in areas such as Vik, Åhus, and Knäbäckshus. The enhanced relationship is due to the smaller elevation changes the closer the GPS dates and DEM years are to each other. Furthermore, transects taken after Babet have a stronger relationship between the RTK-GPS points and DEM values, especially with DEM from 2023 compared to transects taken before Babet (see table 5-7). This further highlights the increase in spatial accuracy when the RTK-GPS points are closer in date to the 2023 DEM. Especially since extreme storm surges contribute to significant changes in elevation.

Tables 5-7 also depict areas with low spatial relationships against both DEM 2023 and 2019. These areas include Kämpinge and Löderup with RTK-GPS points taken on dates 2023-05-02 and 2023-01-19. This is an example of areas where connections with Babet cannot be made due to higher uncertainty. On the other hand, Vik, Falsterbo, Åhus, Kivik, and Skurup have good spatial relationships for both DEMs resulting in more accurate assumptions that can tie these areas to the aftermath of Babet.

5.2 Mitigation Strategies

Referring back to the background chapter 2.2.2, it is evident that the majority of the municipalities have ongoing mitigation and adaptation strategies against erosion and transportation. However, when referring back to the results, it is evident that more suggestions could be made. Municipalities with extensive sandy beaches, such as Ystad, Vellinge, Simrishamn, Skurup, and Kristianstad, should prioritize implementation efforts. In contrast, Bromölla and Sölvesborg, which lack significant sandy coastal areas, should not focus as heavily on these measures. Due to lack of implements from municipalities, many residents near the affected areas have already started building protection barriers in order to protect their homes post Babet (Hallin, et al., 2024). In order to ensure the safety of the infrastructure and residents, nature-based solutions such as the latter mentioned dune restoration, reshaping, and beach nourishments could be implemented. In addition to this, it is evident to combine this with soft strategies, ensuring the availability of shelters, enhanced urban planning, and

implementation of early warning systems. On the other hand, challenges such as lack of local knowledge may arise, meaning that residents may not take the information and early warning systems seriously (Horn, 2015). This highlights the importance of spreading awareness and educating the locals in regard to future storms and flood events. The county board of Scania is aiming at informing concerned municipalities about climate adaptation (Länsstyrelsen Skåne, n.d.). However, the question remains on how well this information reaches the locals. Different campaigns can be implemented to gain the interest of the residents near the affected places. Examples of these could be gardening campaigns, and plantation campaigns. Gray infrastructure in the form of protective barriers should also be considered for areas with elongated sandy beaches susceptible to erosion and accumulation, as well as floodings. As mentioned in chapter 2.2.2, Vellinge and Ystad have ongoing and planned construction of barriers and dikes. This is an effective method mainly against sea level rise and cyclones but also a costly method to implement and monitor. Hence, considerations should be made whether gray infrastructure is a good implementation. This will be discussed further below.

Similarly to gray infrastructure, continuous data collection can help the municipalities with external expertise and possibility to engage in new projects. For example, two 15 meters deep wave buoys in Kämpinge have been set out. The purpose is to collect data on the movement of the waves, which can yield information about the sea's impact on the coast. Based on the data, scientists can further help suggest future climate adaptation measures in Kämpinge (Mikulic, 2024). Other forms of data collection include regular drone flights, on-site measurements, and LiDAR scans as recent data lead to coastal assessments done with higher accuracy. As a result, this can lead to quicker identification of erosion-prone areas, enabling faster implementation of mitigation and adaptation solutions.

Lastly, it is important to note the balancing between the aforementioned solutions as they can contribute to negative outcomes as well. For example, while beach nourishment may lead to reduced erosion in the concerned area, it can also result in increased accumulation in the neighboring areas. The same outcome goes for solutions involving gray infrastructure. Barriers protect the coast from floodings and sediment displacement, but at the same time they can disrupt nearby ecosystems. In contrast, a trade-off should be considered for what would happen if none of the solutions were implemented. Will the high cost of implementation exceed the cost of destruction? For example, SEI (Stockholm Environment Institute), did a case study for Kristianstad municipality proposing methods involving nature-based solutions, green infrastructure, and policy solutions. It was shown that if this project was active today, nature-based solutions such as beach nourishments and dune vegetation could have spared up to 9 m of eroded beach in Kristianstad after Babet (Barquet, 2023).

Site-specific assessments of the coastal area are required in order to evaluate which method provides the best fit from both economic, social, and environmental aspects (Hallin, et al., 2024). For example, site-specific areas such as Anton Fiskares väg and Rörum (see fig. 7-9) experience significant erosion and accumulation. Because these locations are popular tourist

attractions, the presence of gray infrastructure would be unwise. On the other hand, it would be evident to enhance the dune restoration to make the dunes more resilient against storm surges. In order to draw accurate conclusions from site-specific measurements however, the data must be recently collected, which once again highlights the importance of the previous paragraph.

5.3 Limitations

5.3.1 Methodology Regarding Coastal Monitoring

Although the methodology used is straightforward, it is very time consuming. It can also lead to subjectiveness, as identification of dune top and toe is based on interpretation of both numerical and visual data. This interpretation error varies depending on the visibility of dunes in the coastal area. For example, the dune top appeared to be clearer on the coast consisting of sand beaches and less clear in the coast consisting of rocks and pebbles. Besides, some of the coastal areas did not have any sand dunes, as they consist of vegetation and cliffs or concrete. This is especially the case for Bromölla and Sölvesborg municipality as well as areas near towns and villages and can explain the minor change in elevation in these areas. Besides interpretation errors, there are uncertainties in the data as well as some areas yield higher uncertainties than others. Environmental factors such as obscured vision due to shadows, slope, weather conditions, but also calibrations of the scanner can cause some laser points to be absorbed, scattered, and not make it to the surface resulting in interpretation errors (Risbøl & Gustavsen, 2018)

As mentioned before, zoning is a very time-consuming method. Because of this there was no time left for presentation of site-specific analysis throughout the whole study area. Several methods have been created to automate the process of coastal monitoring and minimize interpretation errors. Few examples of these methods are (1)iBluff, (2)CliffMetrics, and (3)CliffDileniaTool, which are custom-made toolboxes focusing on accurately monitoring coastal cliff analysis (1)Plaseanu-Lovejoy, 2023; (2)Payo, et al., 2018; (3)Swirad & Young, 2022). CliffDeliniaTool is a MATLAB/python-based script created by Swirad & Yung (2022). The purpose of CliffDeliniaTool is to accurately identify cliff base and top positions on cross-shore transects (Lysko, et al.,2023; Swirad & Yung, 2022). Similarly, CliffMetrics focuses on delineating cliff top and toe positions, but basing this on geometric characteristics acquired from the digital elevation model (Lysko, et al.,2023; Payo, et al., 2018). iBluff is an R-package specially designed for assessing morphological analysis of coastal bluffs. It can identify bluff tops, toes and other features such as bluff-face (Plaseanu-Lovejoy, 2023). A study conducted by Leutzenburg, et al., (2023) utilized CliffDelinia toolbox in order to identify cliff top and toes from 2007 and 2015 DEM within the entire coastal area of Denmark. Furthermore, the study utilized a cluster analysis using “Spatially Constrained Multivariate Clustering" machine learning tool in ArcGIS in order to detect differences in cliff morphology. This method yields results in a similar way and requires less time.

However, the question arises whether these alternative mentioned methods can identify coastal dunes, which normally do not exceed 20 meters as mentioned in the background. If the latter, another question arises regarding the applicability and accuracy of these methods if no dunes are present. Additionally, it remains uncertain whether these methods yield better results. For instance, the iBluff method requires a digitized polyline of the area between bluff top and toe which once again leads to higher levels of subjectivity. To summarize, there are numerous alternative ways to go around coastal monitoring. As subjectivity and interpretation errors will always arise, the type of method to choose is a matter of suitability for the specified analysis.

5.3.2 Methodology Regarding Map Quality Assessment

It is important to note the uncertainties in the map quality assessment. As RMSE does consider spatial distribution between observed and predicted values, it aids in assessing areas with higher differences between the values hence giving them a value further from 0. However, RMSE does not consider the spatial behavior of the DEMs such as the position and local error autocorrelation (Polidori & Hage, 2020). RMSE is also sensitive to outliers, where larger differences have an overall negative effect on the total value (Chai & Draxler, 2014). It is however believed that the equations susceptibility for outliers is not significant in the results, as the differences between the predicted and observed values are on decimal level.

Quality assessment has been utilized in several other studies, using validation methods such as RMSE and R^2. For example, a study done by Elaksher, et al., (2023) validated the quality of LiDAR through comparing the data with ground survey heights with the help of standard deviation and RMSE. Another study done by Hilgendorf, et al., (2021) aimed to assess biological and morphic changes within foredunes while also evaluating the quality of the data used. The quality assessment methods mentioned in this study included calculating the RMSE of high-resolution terrestrial laser scanning against kite aerial photogrammetry and uncrewed aerial systems. Comparing these studies reveals that RMSE is a popular choice for assessing spatial errors. However, it is often combined with other validation methods. This is also the case in the current study, which combines RMSE with R^2. This approach confirms that while RMSE is sensitive to outliers, it is effective for data quality assessment, especially when combined with other validation methods like R^2 to provide a more comprehensive evaluation of accuracy. Alternative methods for DEMs accuracy assessment include Cohen's Kappa. This method yields a value showcasing if the agreement between the values is better or no better than random chance (McHugh, 2012). This method was considered but not conducted due to considerably low agreements between the DEM and the ground data values which can result in low kappa values.

Another limitation regarding the map quality assessment is the lack of RTK-GPS points. As the acquired transect points covered the entire area, it is still difficult to draw conclusions on DEMs quality and find all the areas where elevation change is more likely to be correlated with Babet. For example, no quality assessment was done for Bromölla and

Sölvesborg municipality, hence, no conclusions can be drawn about DEMs quality in these areas.

As mentioned in chapter 5.3.1, LiDAR data do provide various uncertainties. Everything from obscured vision due to shadows and tilted areas to light absorption. Lastly, since LiDAR scans are typically not conducted continuously throughout the day, it can be challenging to compare them with ground data as factors such as tides and erosion fluctuate frequently. Therefore, these are often not accurate in comparison to the ground measurements taken on the desired day.

5.3.3 Presenting the Results

Given the size of the study area, it is not possible to showcase the volume change in high detail. Maps were made in a way for the reader to get an overview of areas experiencing erosion and accumulation, however it is impossible to present this result in detail without overwhelming the reader with maps. This limitation complicates a detailed interpretation of the results for the reader and makes it challenging for the author to describe their significance. In addition, maps showcasing the hotspot analysis had to be screen captured as the distinction between the colours were not shown as clear when they were exported as layers in ArcGIS. This resulted in poor quality of these images.

5.4 Future studies

This study promotes and proves that it is possible to work on similar assessments with newly generated data. There are, however, possible ways to expand on this. The volume change assessment shows a generalized volume change per municipal border. As previously mentioned, dune morphology and elevation continuously change, leading to various outliers to be present. However, these are generalized when analyzed per municipality. It would be evident to continue conduction of a more detailed analysis focusing on site-specific areas. Suggestions on this can be to merely focus on one municipality in order to gather data with higher accuracy. Alternatively, one can try a semi- or fully automated method for dune top and toe identification as mentioned above, such as iBluff, or CliffDelinia Tool and compare the differences between the manual and automated methods.

Furthermore, the zoning polygons and volume change data can contribute to future analysis regarding Scanias coastal area. For example, it would be interesting to compare the morphology of the area from different years to detect areas more prone to change in the future. It can also be interesting to investigate the projected sea level rise against the volume change analysis. This information can also aid in enhancing resilience within the affected areas. An example of this is depicted in a study by Mehrtens et al., (2023) who investigated coastal dynamics by developing a semi-automated procedure for the remote identification of key dune parameters and performing volume change analysis. The purpose of this analysis was to

correlate the long-term development of coastal dunes with their potential for coastal protection, particularly in the context of projected sea level rise and other climate change-related factors.

Another interesting aspect that could be further explored is whether ongoing mitigation and adaptation measures are effective against larger storm surges, such as Babet. While evaluating these strategies was not the aim of this study, it does touch on this topic to a minor extent. Future research could expand on this by focusing solely on areas where mitigation strategies have been implemented.

6 Summary and Conclusion

The study reveals simultaneous volume changes in dune areas (zone 1) and shoreline plains (zone 2) across the entire study area, confirming the third hypothesis. It is also concluded that Ystad and Skurup municipality have the highest total volume change, while Simrishamn has the lowest in zone 1. Zone 2 shows that Simrishamn experienced the highest amount of accumulation and Kristianstad experienced the highest erosion value. This outcome confirms the first hypothesis stating that municipalities already prone to erosion such as Ystad and Simrishamn will experience the most change. On the other hand, Bromölla and Sölvesborg municipalities demonstrated the lowest total volume change in both zones. These differences can be due to the dynamic and environment of the coastal area, anthropogenic factors, as well as interpretation and data errors, hindering correct interpretation of the dunes. Nonetheless, this result fulfills objectives (1) and (2) as mentioned in the aim chapter 1.1.

While the first and the third hypothesis could be confirmed, the second hypothesis remains inconclusive and could not be fully confirmed nor rejected. Although there is observable significant erosion and accumulation near urban areas, the study lacks comprehensive visualization of all urban settlements within the study area.

The quality of both DEMs is generally good in various places including Falsterbo, Åhus and Kivik, but poor in areas such as Kämpinge and Löderup. This alternation depends on factors such as faults in digital elevation models as well as changes within the coast, such as, tides, sediment displacement from previous storms, and urbanization. The latter fulfills the objective (3) in chapter 1.1.

Lastly, it is concluded that the implementation of mitigation strategies varies depending on the location as well as economic, social, and environmental factors. However, further detailed analysis is needed in order to propose site-specific mitigation strategies. Nevertheless, this study gives a generalized understanding of sediment displacement along the Southern- and Eastern coasts of Scania, Sweden as a result of storm Babet.

7 References

Ahrens C.D. & Henson R. (2018). Meteorology today: an introduction to weather, climate, and the environment. 12th ed, p. 329-330.

Alganci, U., Besol, B. & Sertel, E. (2018). Accuracy Assessment of Different Digital Surface Models. *ISPRS International Journal of Geo-Information,* **7**(3). https://doi.org/10.3390/ijgi7030114

Attal, M., Mudd, S.M., Hurst, M.D., Weinman, B., Yoo, K. & Naylor, K. (2014). Impact of change in erosion rate and landscape steepness on hillslope and fluvial sediments grain size in the Feather River Basin (Sierra Nevada, California). *Earth Surf. Dynam. Discuss*, **2**, p. 1047-1092. 10.5194/esurfd-2-1047-2014

Barquet, K. (2023-11-07). Aftermath of Storm Babet shows the cost of short-term research funding. *Stockholm Environment Institute (SEI).* https://www.sei.org/perspectives/babet-cost-research-funding/

Brandt, A. (2023-10-21). Værste stormflod i over 100 år: Kan nogle steder have været en 500-årshændelse. *DR.* https://www.dr.dk/nyheder/vejret/vaerste-stormflod-i-over-100-aar-kan-nogle-steder-have-vaeret-en-500-aarshaendelse

Costa, P.J.M. (2016). Sediment Transport. *Encyclopedia of Estuaries, Springer, Dordecht.* p. 562-567. https://doi.org/10.1007/978-94-017-8801-4_187

Chai, T. & Draxler, R.R. (2014). Root mean square error (RMSE) or mean absolute error (MAE)?. *Geoscientific Model Development Discussions, Copernicus Publications,* **7**, p. 1525-1534. www.geosci-model-dev-discuss.net/7/1525/2014/

Climate ADAPT. (n.d.). How to factor in uncertainty?. Retrieved 2024-05-18 from: https://climate-adapt.eea.europa.eu/en/knowledge/tools/uncertainty-guidance/topic3

Debaine, F. & Robin, M. (2012). A new GIS modelling of coastal dune protection services against physical coastal hazards. *Ocean & Coastal Management,* **63**, p. 43-54. 10.1016/j.ocecoaman.2012.03.012

Elaksher, A., Ali, T. & Alharthy, A. (2023). A Quantitative Asessment of LIDAR Data Quality. *Remote Sens.*, **15**(2), p. 442. https://doi.org/10.3390/rs15020442

Esri. (n.d.*a*). How Hot Spot Analysis (Getis-Ord Gi*) works – ArcGIS Pro. *Pro.arcgis.com.* Retrieved 2024-05-10 from: https://pro.arcgis.com/en/pro-app/latest/tool-reference/spatial-statistics/h-how-hot-spot-analysis-getis-ord-gi-spatial-stati.htm

Esri. (n.d.*b*). What is a z-score? What is a p-value?. *Pro.arcgis.com.* Retrieved 2023-05-10 from: https://pro.arcgis.com/en/pro-app/latest/tool-reference/spatial-statistics/what-is-a-z-score-what-is-a-p-value.htm

Esko, D., Malmberg Persson, K. & Persson, M., (2000): Quaternary deposits of Skåne, scale 1:250 000. *Sveriges geologiska undersökning Ba 55.* https://resource.sgu.se/dokument/publikation/ba/ba55karta/ba55-karta.pdf

Eyring, V., N.P. Gillett, K.M. Achuta Rao, R. Barimalala, M. Barreiro Parrillo, N. Bellouin, C. Cassou, P.J. Durack, Y. Kosaka, S. McGregor, S. Min, O. Morgenstern, & Y. (2021). In: Human Influence on the Climate System. In Climate Change 2021: The Physical Science Basis. Contribution of Working Group I to the Sixth Assessment Report of the Intergovernmental Panel on Climate Change [Masson-Delmotte, V., P. Zhai, A. Pirani, S.L. Connors, C. Péan, S. Berger, N. Caud, Y. Chen, L. Goldfarb, M.I. Gomis, M. Huang, K. Leitzell, E. Lonnoy, J.B.R. Matthews, T.K. Maycock, T. Waterfield, O. Yelekçi, R. Yu, and B. Zhou (eds.)]. *Cambridge University Press, Cambridge, United Kingdom and New York, NY, USA,* p. 423–552. 10.1017/9781009157896.005.

Fischione, P., Pasquali, D., Celli, D., Di Nucci, C. & Di Risio, M. (2022). Beach drainage System: A Comprehensive Review of a Controversial Soft-Engineering Method. *J. Mar. Sci. Eng.* **10**(2). https://doi.org/10.3390/jmse10020145

Fondriest: Environmental Learning Center. (n.d.). Sediment Transport and Deposition. Retrieved 2024-04-03 from; https://www.fondriest.com/environmental-measurements/parameters/hydrology/sediment-transport-deposition/

Doyle, T.B. & Woodroffe, C.D. (2018). The application of LiDAR to investigate foredune morphology and vegetation. *Geomorphology*, **303**, p. 106-121. https://doi.org/10.1016/j.geomorph.2017.11.005

Hallin, C., Knaggård, Å., Alexanderson, H., Zander, U., Persson, A., Sahlin, U., Wingren, C. & Thorén, H. (2024-02-28). De värsta konsekvenserna av Babet ligger framför oss. *Sydsvenskan.* https://www.sydsvenskan.se/2024-02-28/de-varsta-konsekvenserna-av-babet-ligger-framfor-oss/

Hesp, P.A. & Martínez, M.L. (2007). 7 – Disturbance Processes and Dynamics in Coastal Dunes. *Plant Disturbance Ecology, Academic Press,* p. 215-247. https://doi.org/10.1016/B978-012088778-1/50009-1

Hilgendorf, Z., Marvin, C.M., Turner, C.M. & Walker, I.J. (2021). Assessing Geomorphic Change in Restored Coastal Dune Ecosystems Using a Multi-Platform Aerial Approach. *Remote Sens.*, **13**(3), p. 354. https://doi.org/10.3390/rs13030354

Huertos, M.L. (2020). Chapter 10 - Water Quality and Catchments. *Ecology and Management of Inland Waters: A Californian Perspective with Global Applications.* p. 315-358. https://doi.org/10.1016/B978-0-12-814266-0.00024-6

Horn, D.P. (2015). Chapter 6 – Storm Surge Warning, Mitigation, and Adaptation. In: *Shorder J.F., Ellis, J.T. & Sherman, D.J. Coastal and Marine Hazards, Risks, and Disasters.* P. 153-180. https://doi.org/10.1016/B978-0-12-396483-0.00006-6

International Organization for Standardization (ISO). (2022). Climate Change Adaptation. https://www.iso.org/files/live/sites/isoorg/files/store/en/PUB100449.pdf

IPCC, 2021: Summary for Policymakers. In: Climate Change 2021: The Physical Science Basis. Contribution of Working Group I to the Sixth Assessment Report of the Intergovernmental Panel on Climate Change [Masson-Delmotte, V., P. Zhai, A. Pirani, S.L. Connors, C. Péan, S. Berger, N. Caud, Y. Chen, L. Goldfarb, M.I. Gomis, M. Huang, K. Leitzell, E. Lonnoy, J.B.R. Matthews, T.K. Maycock, T. Waterfield, O. Yelekçi, R. Yu, and B. Zhou (eds.)]. Cambridge University Press, Cambridge, United Kingdom and New York, NY, USA, pp. 3−32, DOI:10.1017/9781009157896.001

Ising, J. (2022). Geologiska förhållanden längs kusten i Skåne, södra Halland och västra Blekinge. *Sveriges Geologiska Undersökning (SGU)*. https://www.sgu.se/globalassets/samhallsplanering/risker/kusterosion-pdf/geologiska-forhallanden.pdf

Joshi, A., Agrawal, S. & Chauhan, P. (2020). Reduction of Atmospheric Effects in Satellite Images During the COVID-19 Induced Lockdown. *J Indian Soc Remote Sens,* **48**, p. 1613-1625. https://doi.org/10.1007/s12524-020-01186-5

Kendon M. (2023-10-26). Storm Babet, 18 to 21 October 2023. *Met Office.* https://www.metoffice.gov.uk/binaries/content/assets/metofficegovuk/pdf/weather/learn-about/uk-past-events/interesting/2023/2023_08_storm_babet.pdf

Kristianstads Kommun. (2024-03-06). Anpassningar till ett förändrat klimat. https://www.kristianstad.se/byggaboochmiljo/klimatochhallbarhetsarbete/klimatochmiljo/anpassningartillettforandratklimat.5849.html

Leutzenburg, G., Bjørk, A.A., Svennevig, K. & Kroon, A. (2023). DRIVERS OF COASTAL CLIFF EROSION IN DENMARK In: Wang, P., Royer, E. & Rosati, J.D. Coastal Sediments 2023. *World Scientific*, p. 1272-1285. https://doi.org/10.1142/9789811275135_0118

Lysko, A., Waćków, W., Forczmański, P., Terefnko, P., Giza, A., b Śledziowski, J., Stępień, G. & Tomszak, A. (2023). CCMORPH – Coastal Cliffs Morphology Analysis Toolbox. *SoftWareX,* **22**, 101386. https://doi.org/10.1016/j.softx.2023.101386

Länsstyrelsen Skåne. (n.d.). Klimatanpassning. Retrieved 2024-05-10 from: https://www.lansstyrelsen.se/skane/samhalle/klimatanpassning.html

Martínez, M.L., Hesp, P.A. & Gallego-Farnández, J.B. (2013). Coastal Dunes: Human Impact and Need for Restoration In: Martínez, M., Gallego-Fernández, J., Hesp, P. (eds) Restoration of Coastal Dunes. *Springer Series on Environmental Management*. Springer, Berlin, Heidelberg. P. 1–14. https://doi.org/10.1007/978-3-642-33445-0_1

Mikulic, B. (2024-05-16). Så hjälper vågbojar forskarna att rädda sydkusten. *SVT nyheter.*
https://www.svt.se/nyheter/lokalt/skane/sa-hjalper-vagbojar-forskarna-att-radda-sydkusten

McDonald, R.E. (2011). Understanding the impact of climate change on Northern Hemisphere extra-tropical cyclones. *Climate Dynamics, Springer* **37,** p. 1399-1425. https://doi.org/10.1007/s00382-010-0916-x

McHugh, M. (2012). Interrater reliability: the kappa statistic. *Biochem Med (Zagreb)* **22(**3), p. 276-282. https://www.ncbi.nlm.nih.gov/pmc/articles/PMC3900052/

Mehrtens, B., Lojek, O., Kosmalla, V., Bölker, T. &Goseberg, N. (2023). Foredune growth and storm surge protection potential at the Eiderstedt Peninsula, Germany. *Frontiers in Marine Science*, **9,** https://doi.org/10.3389/fmars.2022.1020351

Mendelsohn, R. & Zheng, L. (2020). Coastal Resilience Against Storm Surge from Tropical Cyclones. *Atmosphere*, **11**(7). https://doi.org/10.3390/atmos11070725

State of Florida, Department of Environmental Protection. (n.d.). Building Back the Sand Dunes. Retrieved 2023-05-03 from: https://floridadep.gov/sites/default/files/Building%20Back%20The%20Sand%20Dunes_02.06.17_0.pdf

Mitchell, S.B. (2020). Chapter 30 - Sediment Transport and Marine Protected Areas. *Marine Protected Areas; Science, Policy and Management, Elsevier.* p. 587-598. https://doi.org/10.1016/B978-0-08-102698-4.00030-7

National Oceanic and Atmospheric Administration (NOAA). (2023-01-20). What is Lidar?. https://oceanservice.noaa.gov/facts/lidar.html

Naturvårdsverket. (2023-11-03). Nationella maRTKäckedata (NMD). https://www.naturvardsverket.se/veRTKyg-och-tjanster/kartor-och-karttjanster/nationella-maRTKackedata/

Olaoluwa, E.E., Durowoju, O.S., Orimoloye, I.R., Daramola, M.T., Ayobami, A.A. & Olorunsaye, O. (2022). 2.4.4 **E**xtratropical-Cyclones In: Ongoma, V. & Tabari, H. Climate Impacts on Extreme Weather. P. 1-17. https://www.sciencedirect.com/topics/earth-and-planetary-sciences/extratropical-cyclone

Olumide, S. (2023-08-08). Root Mean Square Error (RMSE) in AI: What You Need To Know. *Arize*. https://arize.com/blog-course/root-mean-square-error-rmse-what-you-need-to-know/

Payo, A., Antelo, B.J., Hurst, M., Plaseanu-Lovejoy, M., Williams, C., Jenkins, G., Lee, K., Favis-Mortlock, D., Barkwith, A. & Ellis, M.A. (2018). Development of an automatic delineation of cliff top and toe on very irregular planform coastlines (CliffMetrics v1.0). *Geosci. Model Dev.* **11**(10), p. 4317-4337. https://doi.org/10.5194/gmd-11-4317-2018

Persson, G., Sjökvist, E., Åström, S., Eklund, D., Andréasson, J., Johnell, A., Asp, M., Olsson, J., Nerheim, S. (2012-02-24). Klimatanalys för Skåne Län. *SMHI*. Report no. 2011-52. https://www.lansstyrelsen.se/download/18.2e0f9f621636c84402730f3d/1528811635925/LSTM-SMHI_2012_Klimatanalys%20f%C3%B6r%20Sk%C3%A5ne%20l%C3%A4n.pdf

Plaseanu-Lovejoy, M. (2023). iBluff: an open-source R package for geomorphic analysis of coastal bluffs/cliffs. *SoftwareX,* **21**. 101325. https://doi.org/10.1016/j.softx.2023.101325

Polidori, L. & El Hage, M. (2020). Digital Elevation Model Quality Assessment Methods: A Critical Review. *Remote Sens,* **12**(21). https://doi.org/10.3390/rs12213522

Provoost, S., Laurence, M., Jones, M. & Edmondson, S.E. (2009). Changes in landscape and vegetation of coastal dunes in northwest Europe: a review. *Journal of Coastal Conservation, Springer* **15**, p. 207-226. https://doi.org/10.1007/s11852-009-0068-5

Pähtz, T., Clark, A.H., Valyrakis, M. & Durán, O. (2020). The Physics of Sediment Transport Initiation, Cessation, and Entrainment Across Aeolian and Fluvial Environments. *Reviews of Geophysics* **58**(1). https://doi.org/10.1029/2019RG000679

Ranson, M., Kousky, C., Ruth, M., Jantarasami, L., Crimmins, A. & Traquinio, L. (2014). Tropical and extratropical cyclone damages under climate change. *Climatic Change* **27**, p. 227-241. https://doi.org/10.1007/s10584-014-1255-4

Risbøl, O. & Gustavsen, L. (2018). LiDAR from drones employed for mapping archaeology – Potential, benefits and challenges. *Archaeological Prospection,* **25**(4), p. 329-338. https://doi.org/10.1002/arp.1712

RISC-KIT. (n.d.). Grey Infrastructure. Retrieved 2024-05-10 from: https://www.coastal-management.eu/taxonomy/term/67.html

SandLife. (n.d.). "Habitat types and species". Retrieved 2023-05-03 from: https://sandlife.se/?page_id=801

Shinn, Y.J., Chough, C.H., Kim, J.W. & Woo, J. (2007). Development of depositional systems in the southeastern Yellow Sea during the postglacial transgression. *Marine Geology, Elsevier* **239**(1-2), p. 59-82. https://doi.org/10.1016/j.margeo.2006.12.007

Siegel, F.R. (2020). Structures That Protect Coastal Populations, Assets, and GDPs: Sea Dikes, Breakwaters, Seawalls. *Adaptation of Coastal Cities to Global Warming, Sea Level Rise, Climate Change and Endemic Hazards,* p. 11-25. https://doi.org/10.1007/978-3-030-22669-5_3

Sigren, J.M., Figlus, J. & Armitage, A. R. (2014). Coastal sand dunes and dune vegetation: Restoration, erosion, and storm protection. *Shore & Beach,* **82**(4). https://www.researchgate.net/publication/270822597_Coastal_sand_dunes_and_dune_vegetation_Restoration_erosion_and_storm_protection

Simrishamn Kommun. (2024–04-04*a*). Åtgärder efter stormarna i Simrishamns Kommun.
https://www.simrishamn.se/gata-park-och-natur/atgarder-efter-stormarna-i-simrishamns-kommun

Simrishamn Kommun. (2024-03-27*b*). Badstranden vid Rörum/Knäbäckshusen avstängd 2024. https://www.simrishamn.se/gata-park-och-natur/park-och-natur/badstrander/badstranden-vid-rorum-knabackshusen-avstangd-2024

SMHI. (2023-11-13*a*). Oktober 2023 – Stormen Babet gav höga vågor och vattenstånd. https://www.smhi.se/klimat/klimatet-da-och-nu/manadens-vader-och-vatten-sverige/tillstandet-i-sveriges-hav/oktober-2023-stormen-babet-gav-hoga-vagor-och-vattenstand-1.200473?l=null

SMHI. (2023-11-28*b*). ”Anti-Babet” tömde sydkusten på vatten. https://www.smhi.se/bloggar/vaderleken-2-3336/anti-babet-tomde-sydkusten-pa-vatten-1.202369

Statens Geotekniska Institut (SGI). (2023-07-09*a*). Om oss. https://www.sgi.se/sv/om-sgi/

Statens Geotekniska Institut (SGI). (2023–10-24*b*). Kraftig Stranderosion i Skåne – byggnader rasade i havet. https://press.sgi.se/posts/news/kraftig-stranderosion-i-skane---byggnader-ras

Statens Geotekniska Institut (SGI). (2024-01-07*a*). Erosionsdrabbade kuster dokumenteras med laserskanning. https://press.sgi.se/posts/news/erosionsdrabbade-kuster-dokumenteras-med-lase

Statens Geotekniska Institut (SGI). (2024-04-18*b*). Före och efter stormen Babet – unika bilder avslöjar extrem stranderosion. https://www.svt.se/nyheter/inrikes/ny-unik-kartlaggning-extrem-stranderosion-i-skane-efter-stormen-babet

Sveriges Geologiska Undersökning (SGU). (2020-04-07). Översikt av Sveriges stranderosion. https://www.sgu.se/samhallsplanering/risker/stranderosion/oversikt-stranderosion-sverige/

Swirad, Z.M. & Young, A.P. (2022). CliffDeliniaTool v1.2.0: an algorithm for identifying coastal cliff base and top positions. *Geosc. Model Dev.* **15**(4), p. 1499-1512. https://doi.org/10.5194/gmd-15-1499-2022

The Geological Society. (n.d). Erosion and Transport. Retrieved 2024-04-25 from: https://www.geolsoc.org.uk/ks3/gsl/education/resources/rockcycle/page3462.html

Trelleborgs Kommun. (2023-10-19*a*). Vall som kustskydd godkänd – första steget mot förverkligande av Västra Sjöstaden. https://www.trelleborg.se/nyheter/vall-som-kustskydd-godkand-forsta-steget-mot-forverkligande-av-vastra-sjostaden/

Trelleborgs Kommun. (2023–10-23*b*). Kustskydd i Trelleborg. https://www.trelleborg.se/bygga-bo-miljo/samhallsutveckling-och-hallbarhet/klimat-och-miljo/kustskydd-i-trelleborg/

Trelleborgs Kommun. (2023-12-29*c*). Efter stormen: frågor och svar. https://www.trelleborg.se/bygga-bo-miljo/samhallsutveckling-och-hallbarhet/klimat-och-miljo/kustskydd-i-trelleborg/efter-stormen-fragor-och-svar/

Turowski, J.M., Rickenmann, D. & Dadson, S.J. (2010). The partitioning of the total sediment load of a river into suspended load and bedload: a review of empirical data. *Sedimentology* **57**(4), p. 1126-1146. https://doi.org/10.1111/j.1365-3091.2009.01140.x

U.S climate resilience toolkit. (2024-05-10). Restoring natural dunes to enhance coastal protection. https://toolkit.climate.gov/case-studies/restoring-natural-dunes-enhance-coastal-protection

United States Geological Survey (USGS). (n.d.). Aerial photograph vs. orthoimage. Retrieved 2023-04-04 from: https://www.usgs.gov/media/images/aerial-photograph-vs-orthoimage

Vellinge Kommun. (2019). Kustprogram. Report no. 2019/387. https://vellinge.se/siteassets/planer-och-projekt-i-vellinge-kommun/dokument/kustprogrammet/kustprogram_antagen-kf20200928.pdf

Ystad Kommun. (2024-04-25). Olika sätt att skydda kusten. https://www.ystad.se/bygg-miljo/miljo-och-avfall/natur-miljo-och-klimat2/klimatanpassning/integrerad-kustzonsforvaltning/kustskydd1/

Österlen Syd. (n.d). Stranderosionen. Retrieved 2024-05-03 from: https://osterlensyd.se/stranderosionen/

8 Appendix

8.1 HotSpot Analysis of Maps

Referring back to chapter 5.3.3, it is hard to present the hotspot analysis across the whole study area. In order to not overwhelm the reader with many maps, they were moved to the appendix. The following maps in chapter 8.1 cover each municipality with 3 zoomed in example areas showing the hotspot analysis. The maps try to capture the analysis in both urban and natural surroundings.

Appendix 1: Illustration of HotSpot analysis over Vellinge municipality

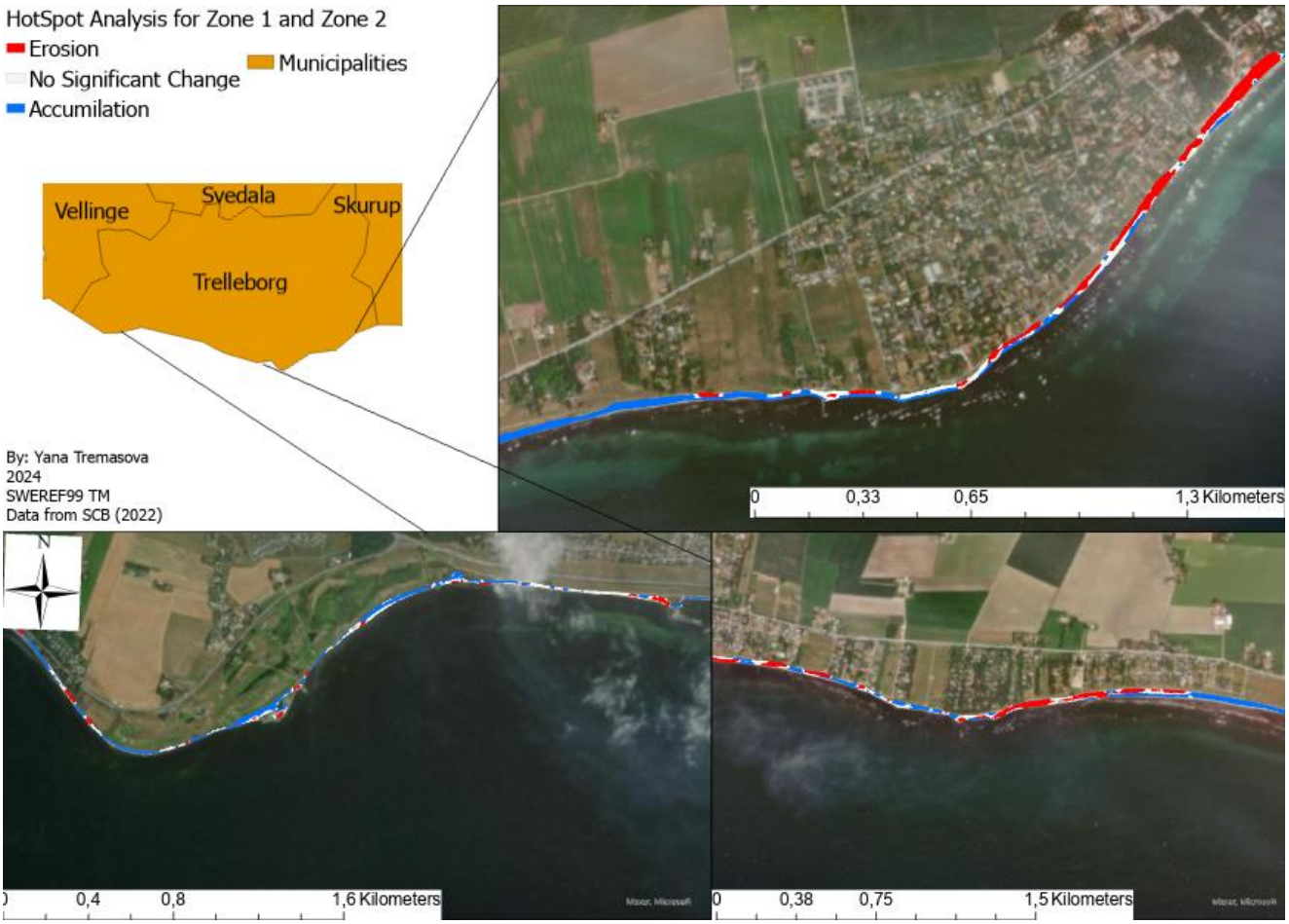

Appendix 2: Illustration of HotSpot analysis over Trelleborg municipality

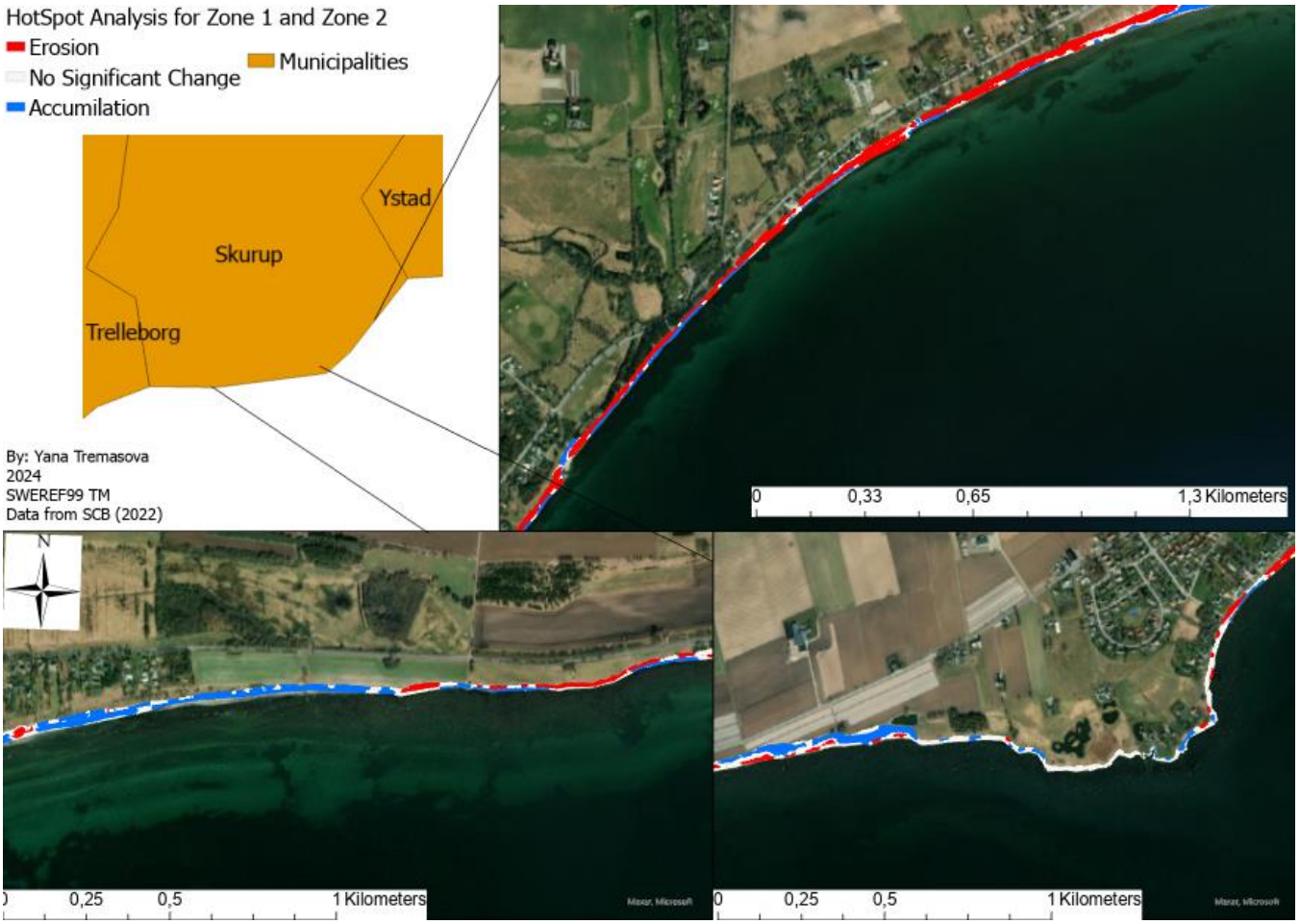

Appendix 3: Illustration of HotSpot analysis over Skurup municipality

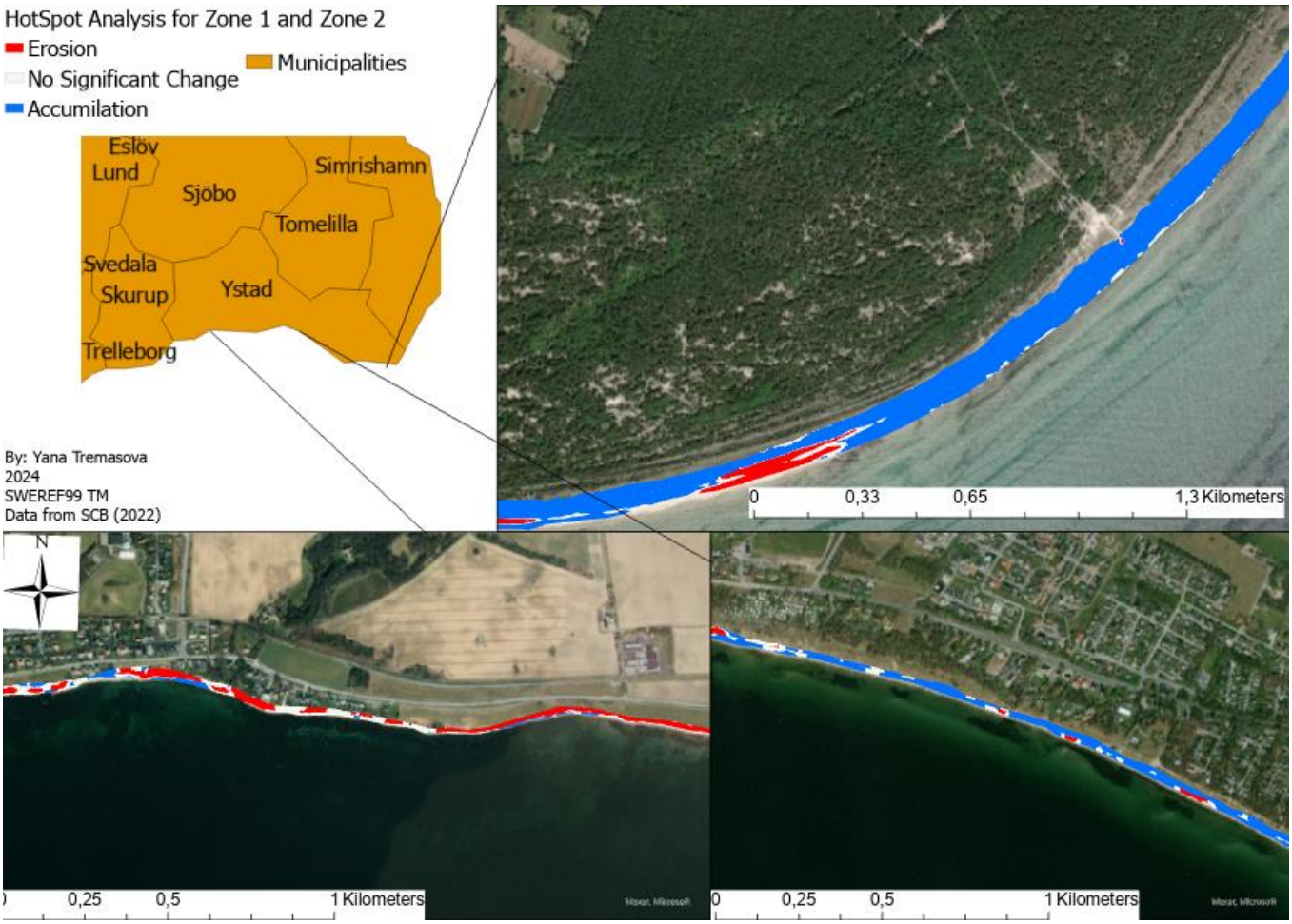

Appendix 4: Illustration of HotSpot analysis over Ystad municipality

Appendix 5: Illustration of HotSpot analysis over Simrishamn municipality

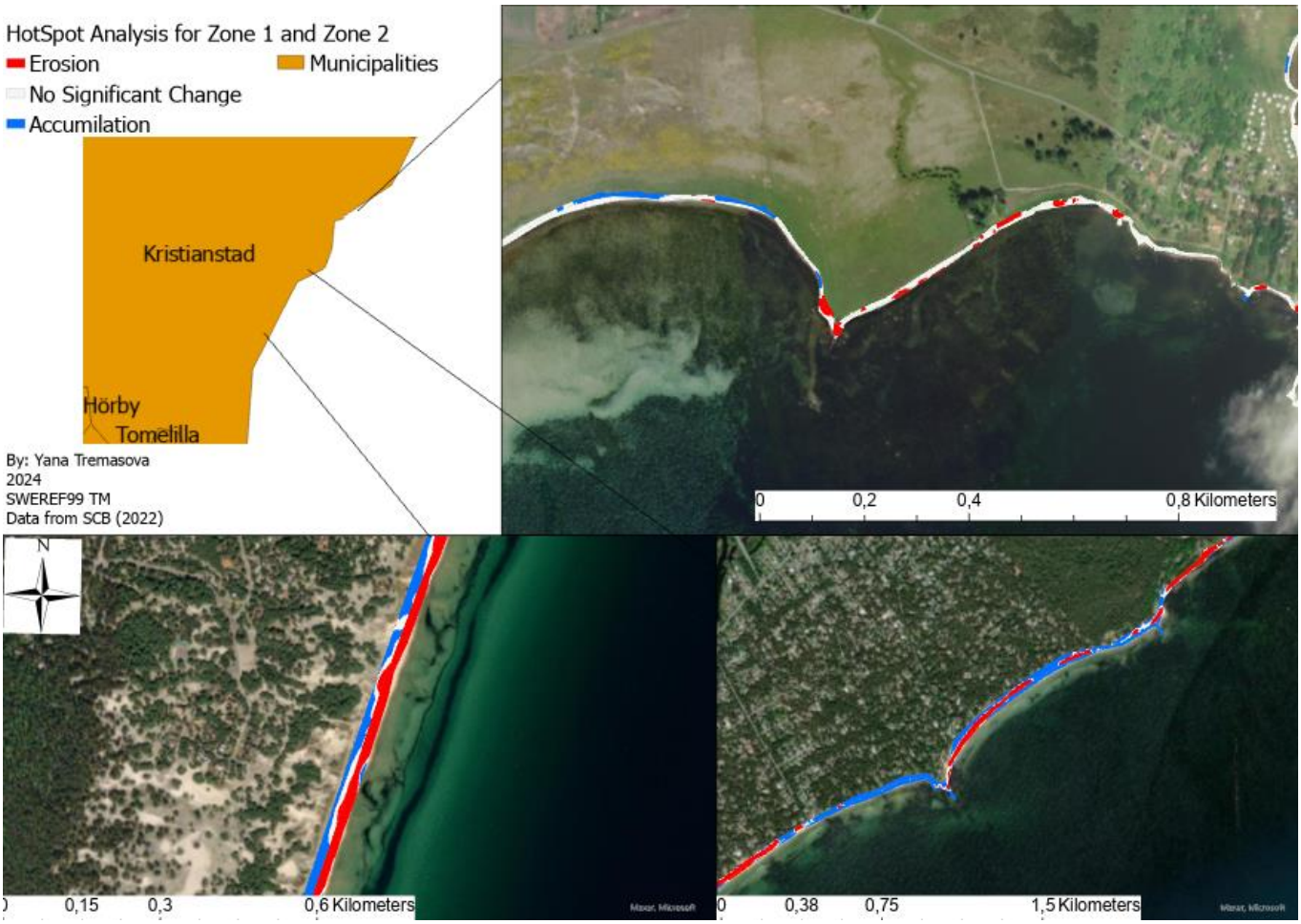

Appendix 6: Illustration of HotSpot analysis over Kristianstad municipality

Appendix 7: Illustration of HotSpot analysis over Bromölla municipality

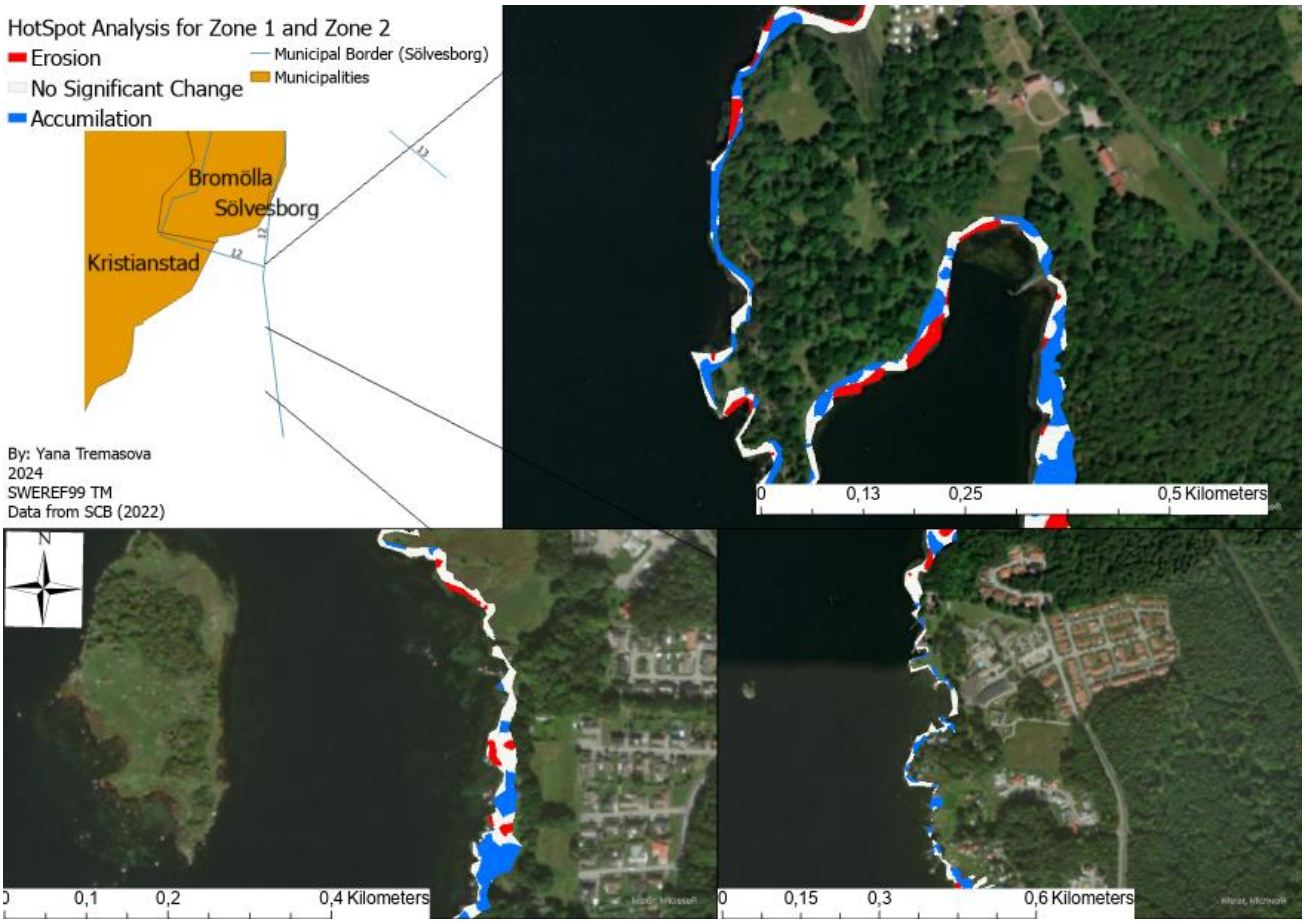

Appendix 8: Illustration of HotSpot analysis over Sölvesborg municipality

8.2 Scatter Plots

Following the same reasoning as chapter 8.1, this chapter presents scatterplots done against each GPS point (see table 2). These scatterplots are created to visually illustrate the locations of outliers for each DEM, helping the reader understand the distribution and anomalies in the data.

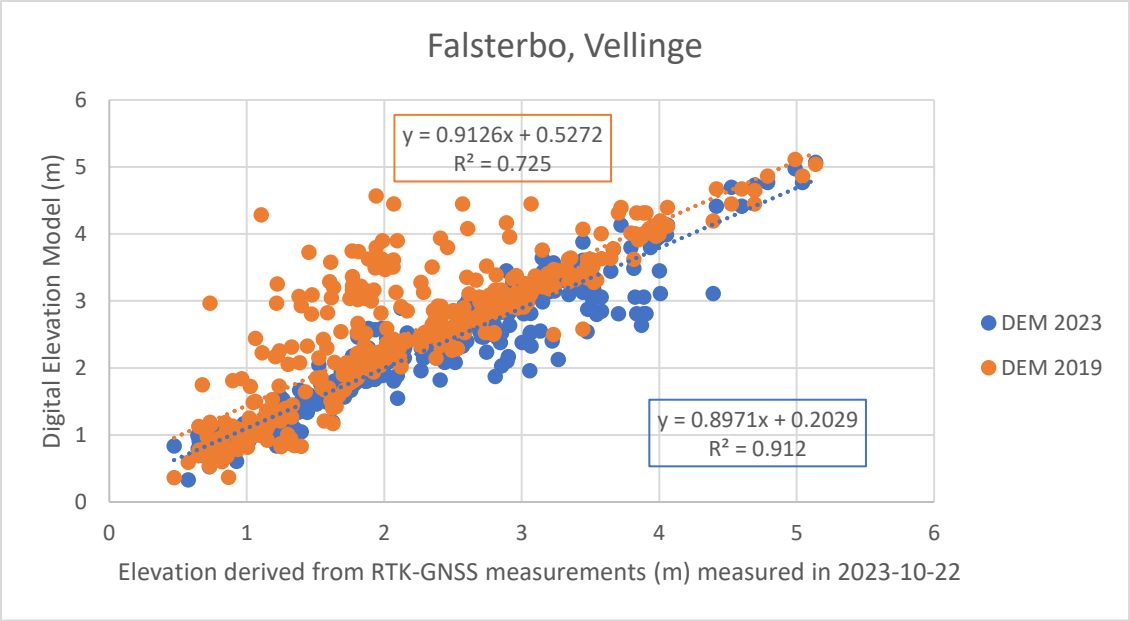

Appendix 9: Scatter Plot depicting the relationship between predicted values (DEM) against observed values (RTK-GNSS) in Falsterbo, Vellinge. The linear dotted lines represent the best fitted straight line between the predicted and observed values for each year respectively. Ground data measured in 2023-10-22.

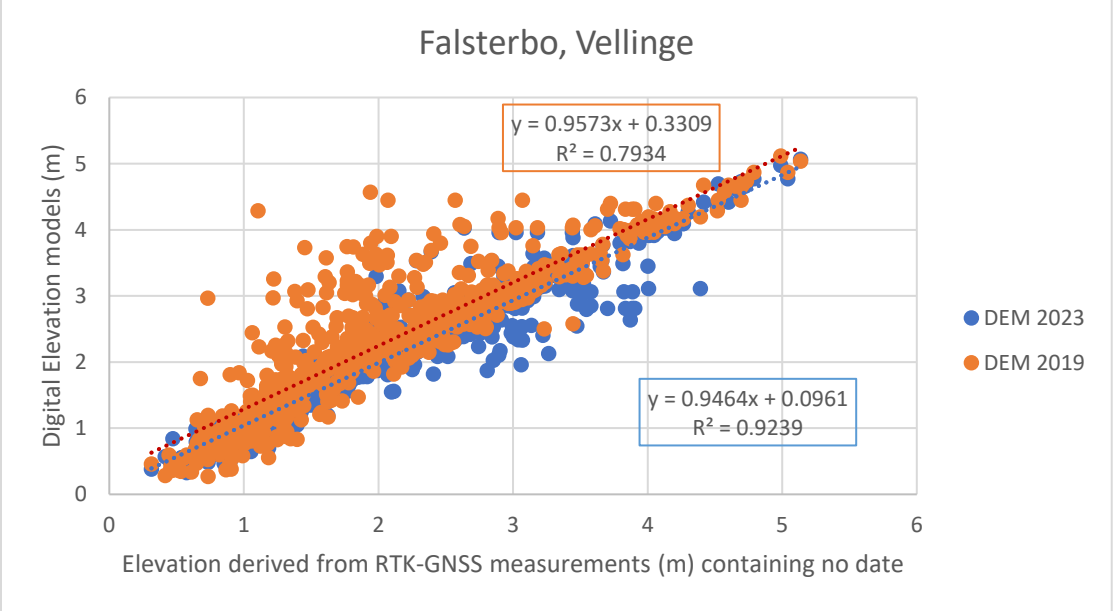

Appendix 10: Scatter Plot depicting the relationship between predicted values (DEM) against observed values (RTK-GNSS) in Falsterbo, Vellinge. The linear dotted lines represent the best fitted straight line between the predicted and observed values for each year respectively. No date for when ground data was measured.

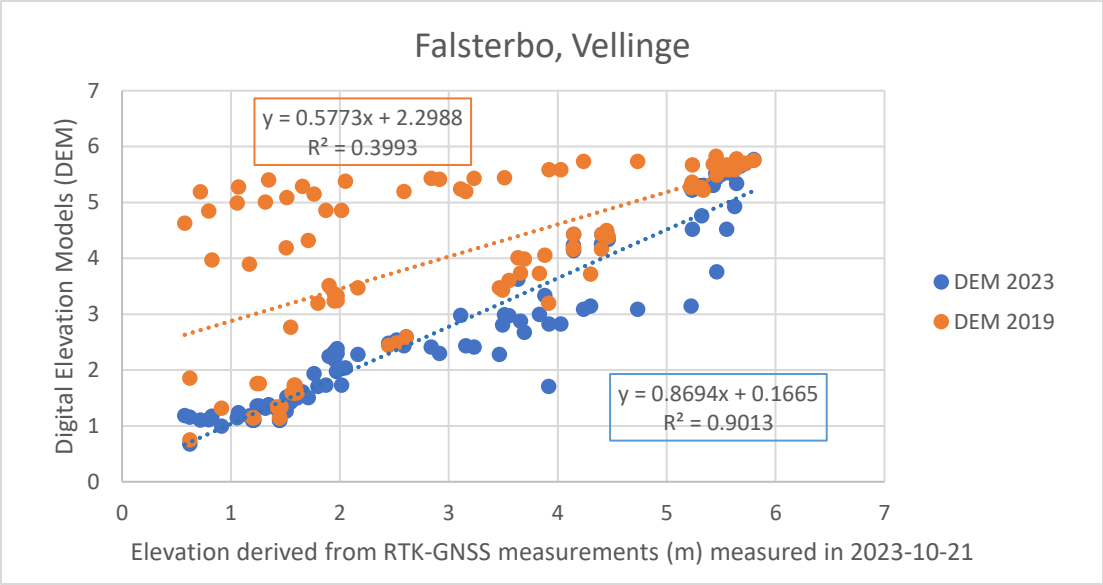

Appendix 11: Scatter Plot depicting the relationship between predicted values (DEM) against observed values (RTK-GNSS) in Falsterbo, Vellinge. The linear dotted lines represent the best fitted straight line between the predicted and observed values for each year respectively. Ground data measured in 2023-10-21.

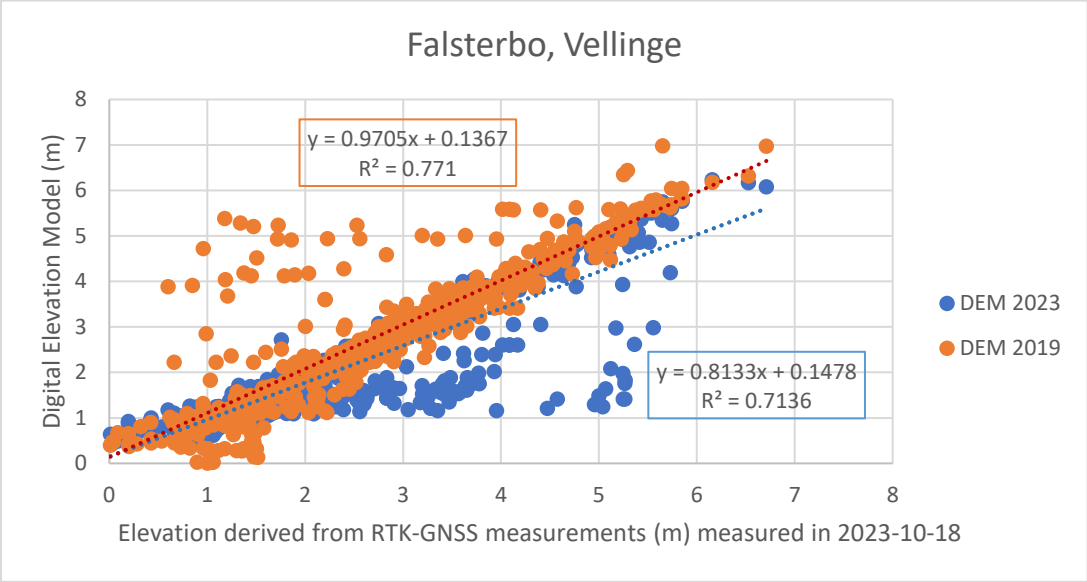

Appendix 12: Scatter Plot depicting the relationship between predicted values (DEM) against observed values (RTK-GNSS) in Falsterbo, Vellinge. The linear dotted lines represent the best fitted straight line between the predicted and observed values for each year respectively. Ground data measured in 2023-10-18.

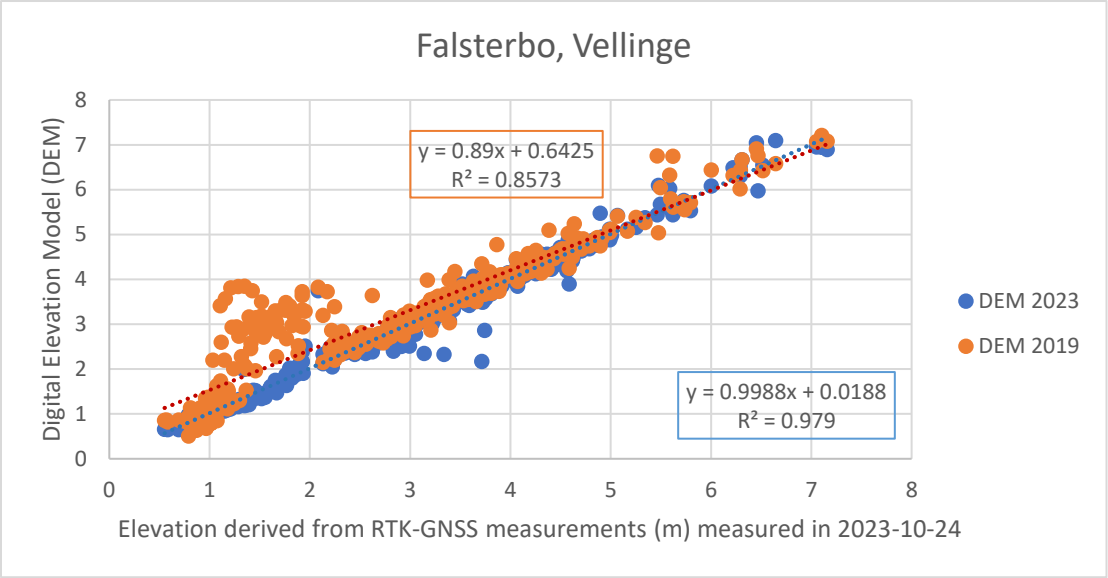

Appendix 13: Scatter Plot depicting the relationship between predicted values (DEM) against observed values (RTK-GNSS) in Falsterbo, Vellinge. The linear dotted lines represent the best fitted straight line between the predicted and observed values for each year respectively. Ground data measured in 2023-10-24.

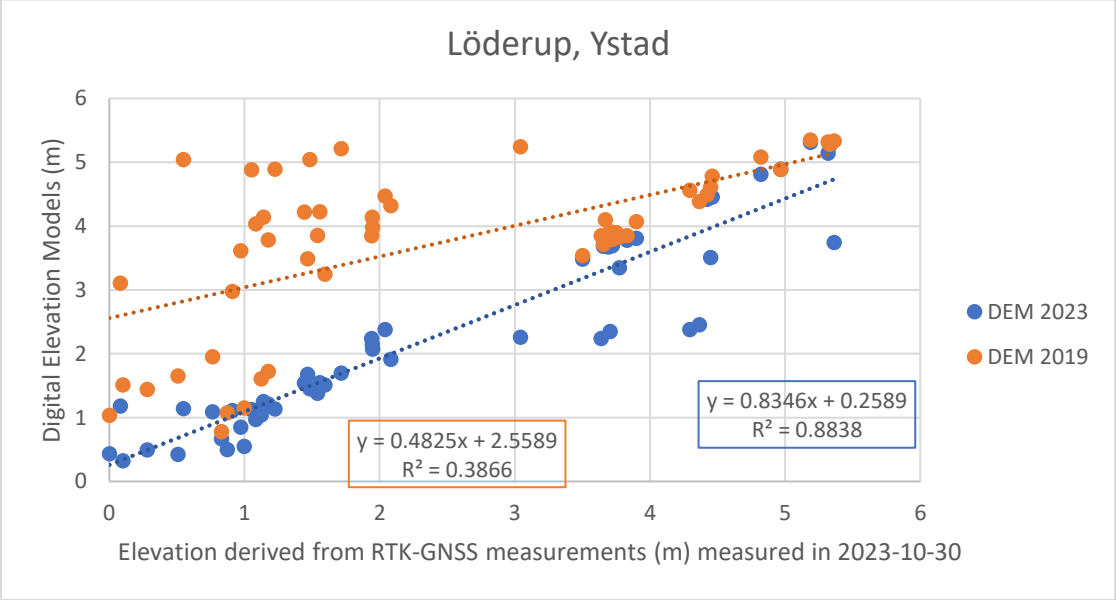

Appendix 14: Scatter Plot depicting the relationship between predicted values (DEM) against observed values (RTK-GNSS) in Löderup. The linear dotted lines represent the best fitted straight line between the predicted and observed values for each year respectively. Ground data measured in 2023-10-30.

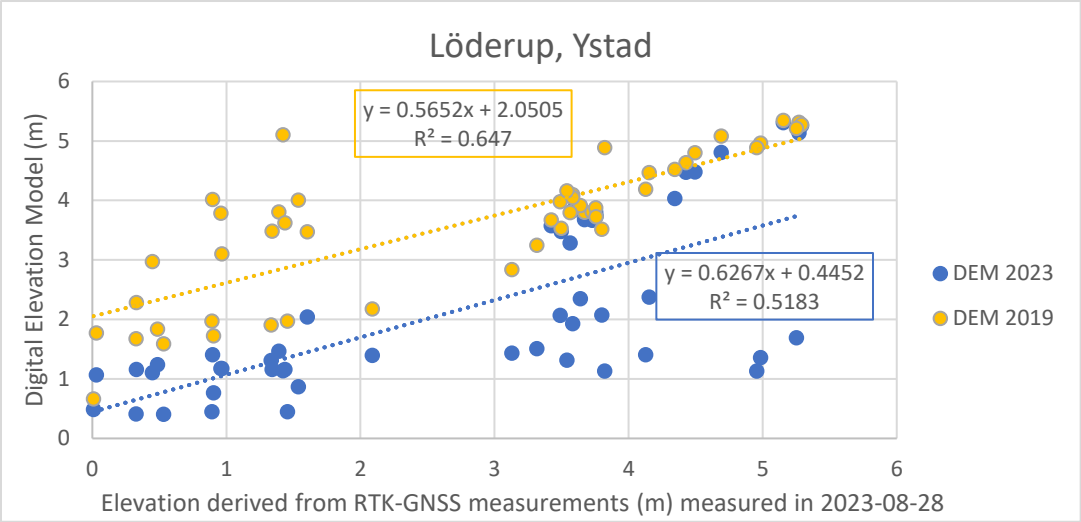

Appendix 15: Scatter Plot depicting the relationship between predicted values (DEM) against observed values (RTK-GNSS) in Löderup, Ystad. The linear dotted lines represent the best fitted straight line between the predicted and observed values for each year respectively. Ground data measured in 2023-08-28.

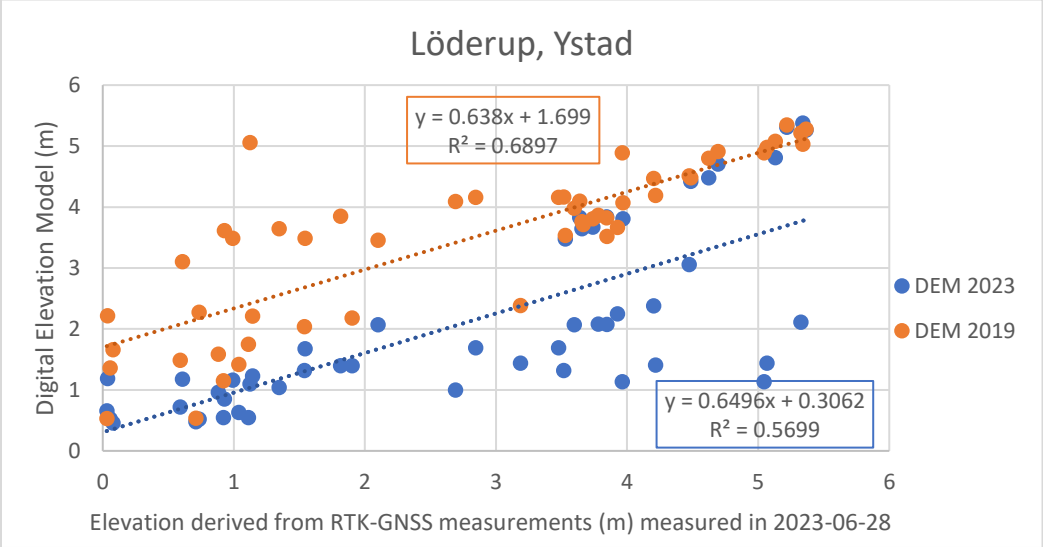

Appendix 16: Scatter Plot depicting the relationship between predicted values (DEM) against observed values (RTK-GNSS) in Löderup, Ystad. The linear dotted lines represent the best fitted straight line between the predicted and observed values for each year respectively. Ground data measured in 2023-06-28.

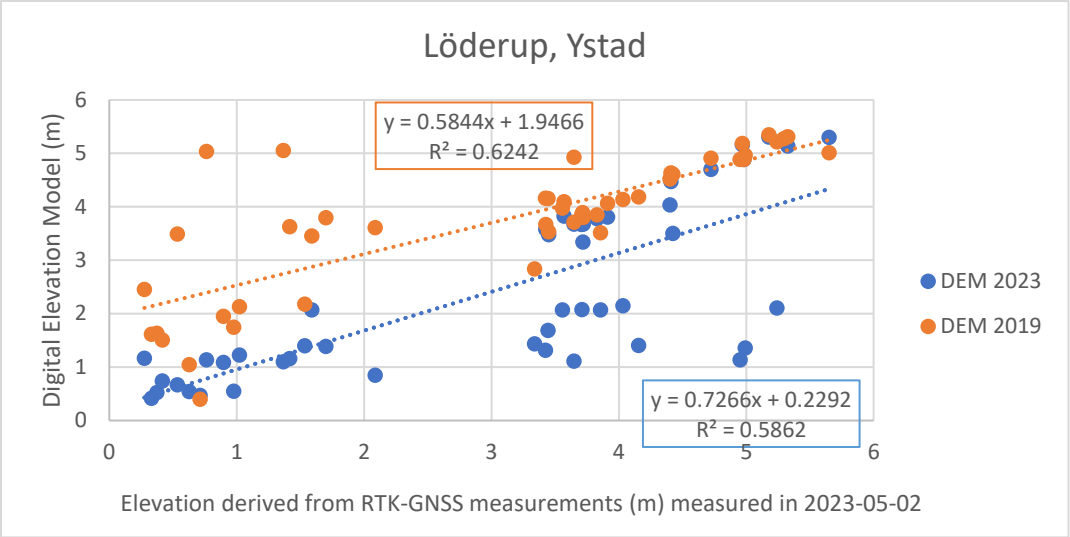

Appendix 17: Scatter Plot depicting the relationship between predicted values (DEM) against observed values (RTK-GNSS) in Löderup, Ystad. The linear dotted lines represent the best fitted straight line between the predicted and observed values for each year respectively. Ground data measured in 2023-05-02.

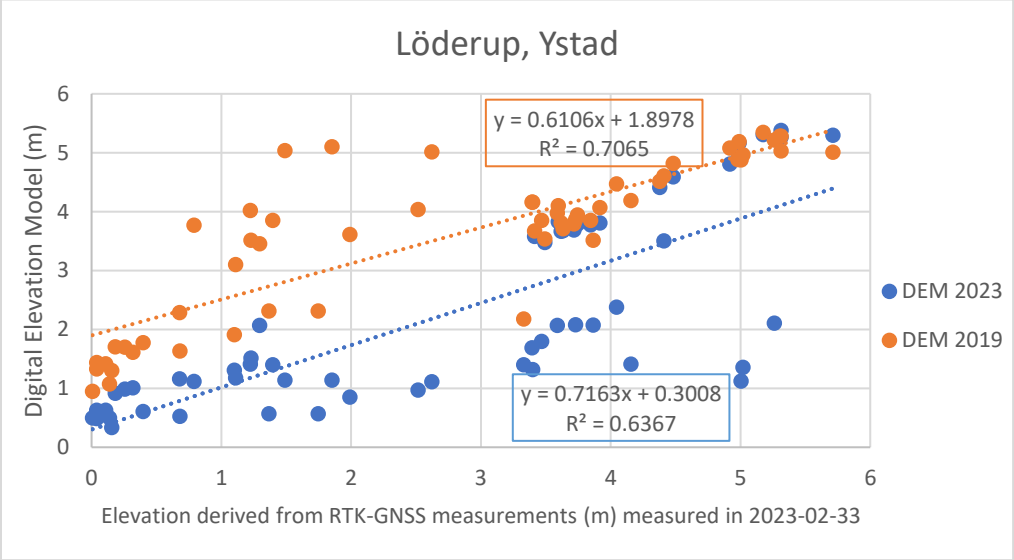

Appendix 18: Scatter Plot depicting the relationship between predicted values (DEM) against observed values (RTK-GNSS) in Löderup, Ystad. The linear dotted lines represent the best fitted straight line between the predicted and observed values for each year respectively. Ground data measured in 2023-02-23.

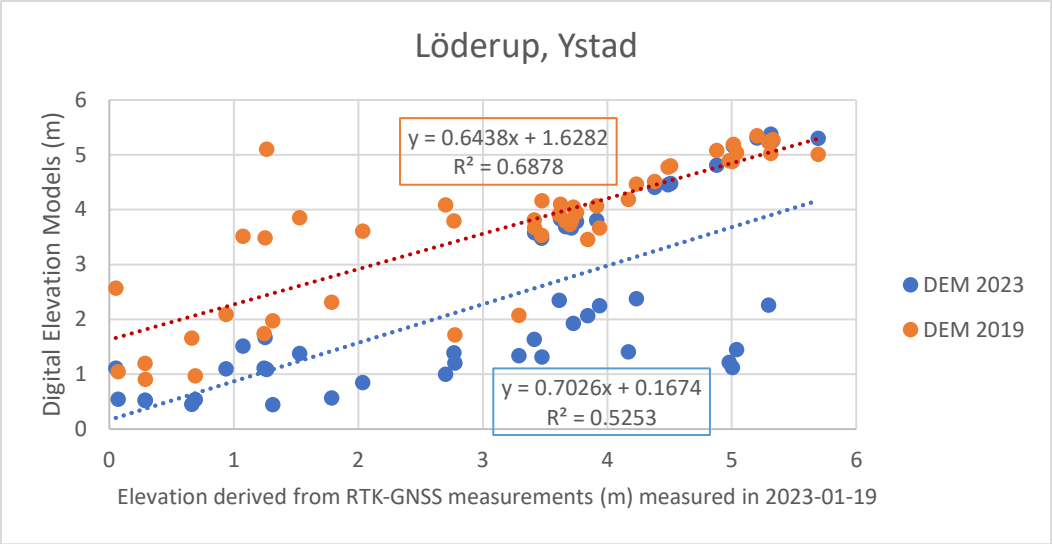

Appendix 19: Scatter Plot depicting the relationship between predicted values (DEM) against observed values (RTK-GNSS) in Löderup, Ystad. The linear dotted lines represent the best fitted straight line between the predicted and observed values for each year respectively. Ground data measured in 2023-01-19.

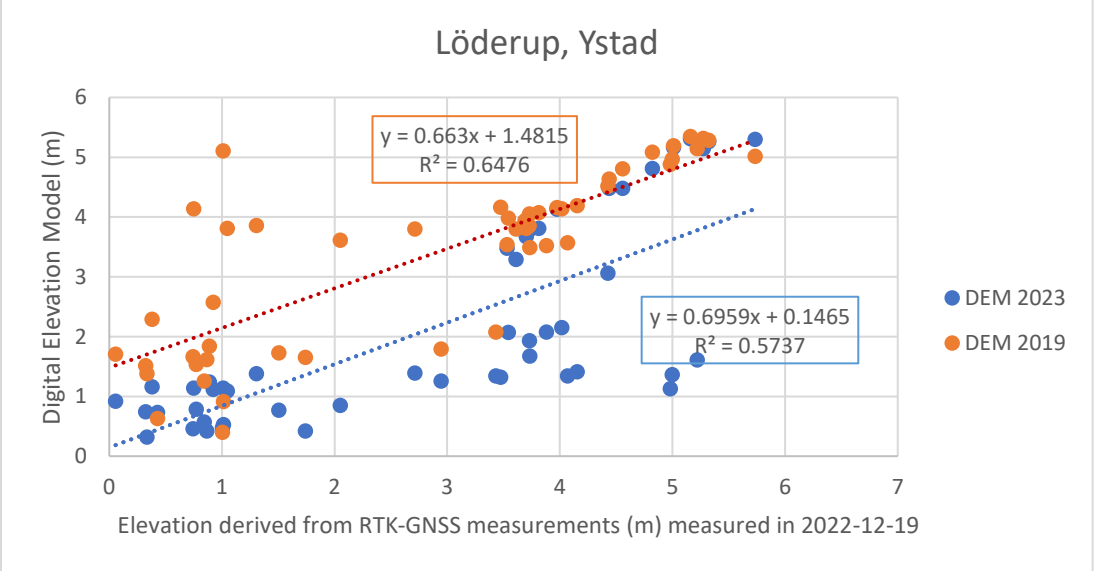

Appendix 20: Scatter Plot depicting the relationship between predicted values (DEM) against observed values (RTK-GNSS) in Löderup, Ystad. The linear dotted lines represent the best fitted straight line between the predicted and observed values for each year respectively. Ground data measured in 2022-12-19.

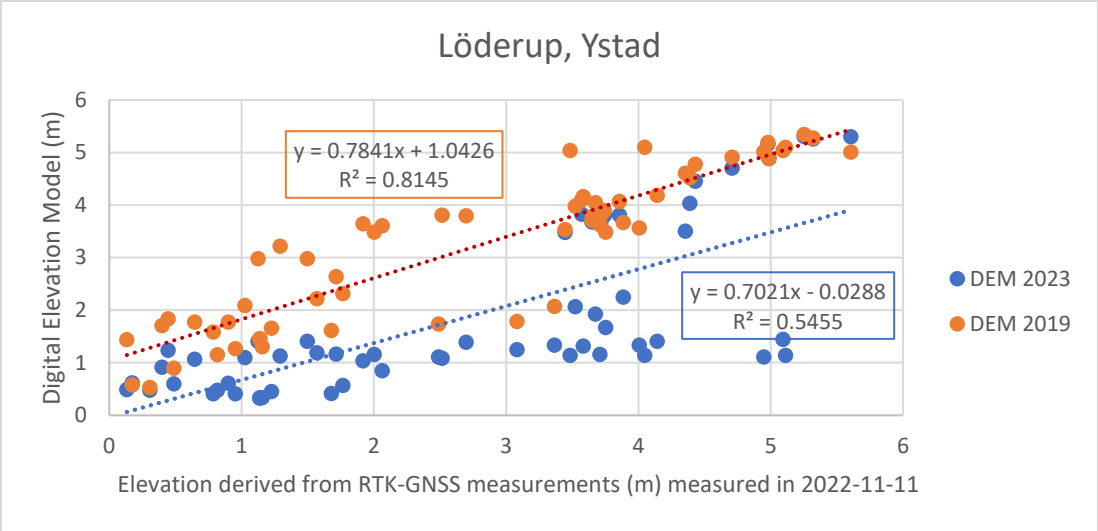

Appendix 21: Scatter Plot depicting the relationship between predicted values (DEM) against observed values (RTK-GNSS) in Löderup, Ystad. The linear dotted lines represent the best fitted straight line between the predicted and observed values for each year respectively. Ground data measured in 2022-11-11.

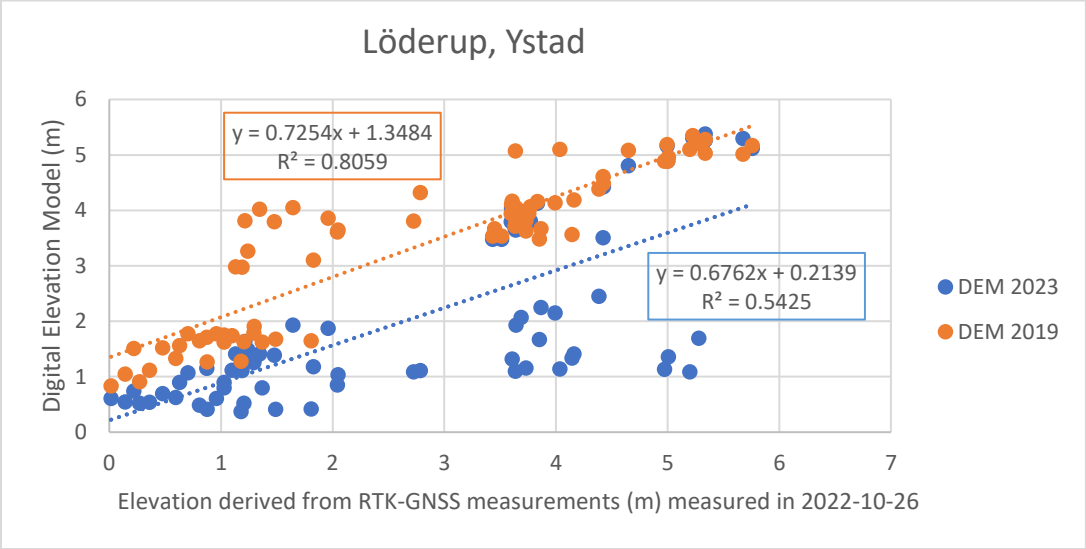

Appendix 22: Scatter Plot depicting the relationship between predicted values (DEM) against observed values (RTK-GNSS) in Löderup, Ystad. The linear dotted lines represent the best fitted straight line between the predicted and observed values for each year respectively. Ground data measured in 2022-10-26.

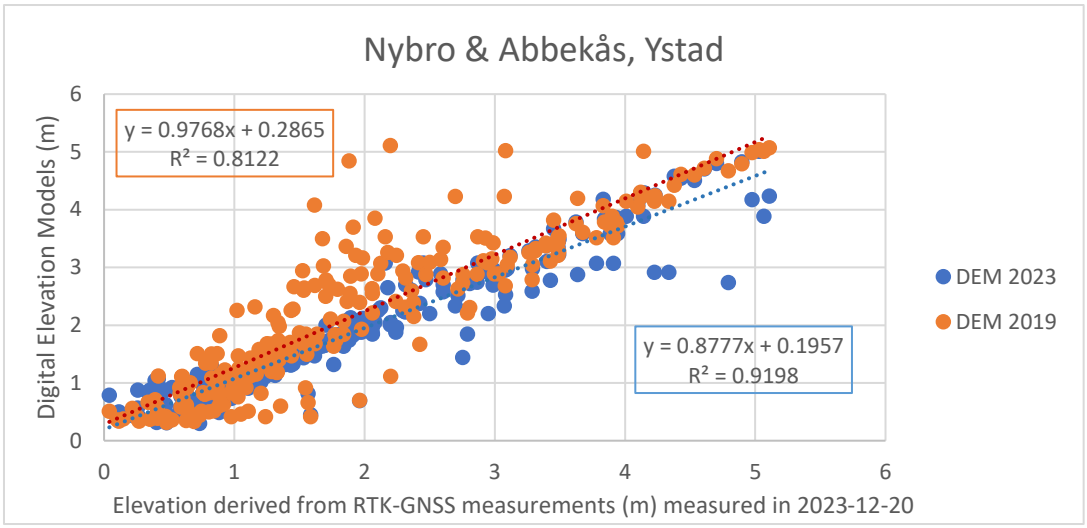

Appendix 23: Scatter Plot depicting the relationship between predicted values (DEM) against observed values (RTK-GNSS) in Nybrostrand & Abbekås, Ystad. The linear dotted lines represent the best fitted straight line between the predicted and observed values for each year respectively. Ground data measured in 2023-12-20.

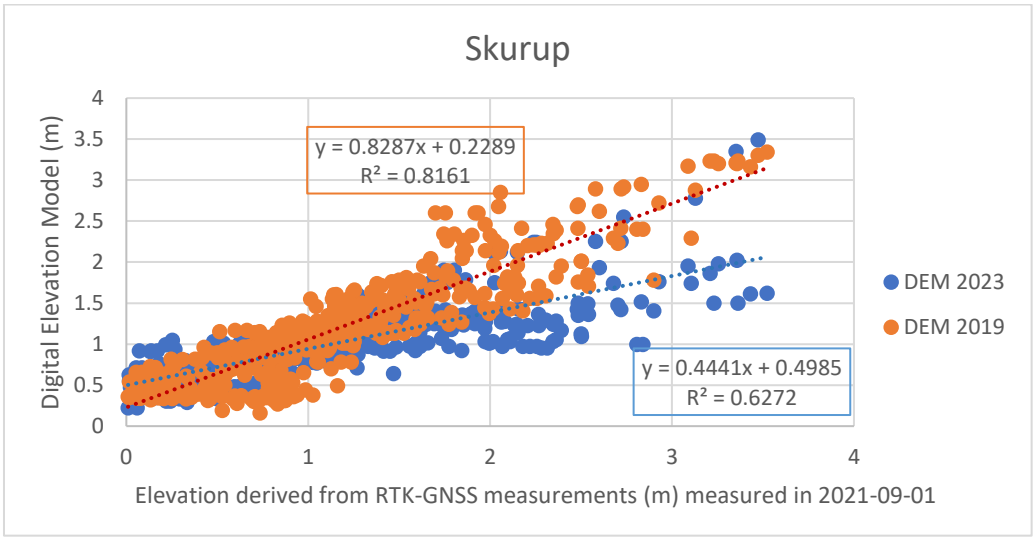

Appendix 24: Scatter Plot depicting the relationship between predicted values (DEM) against observed values (RTK-GNSS) in Skurup. The linear dotted lines represent the best fitted straight line between the predicted and observed values for each year respectively. Ground data measured in 2021-09-01.

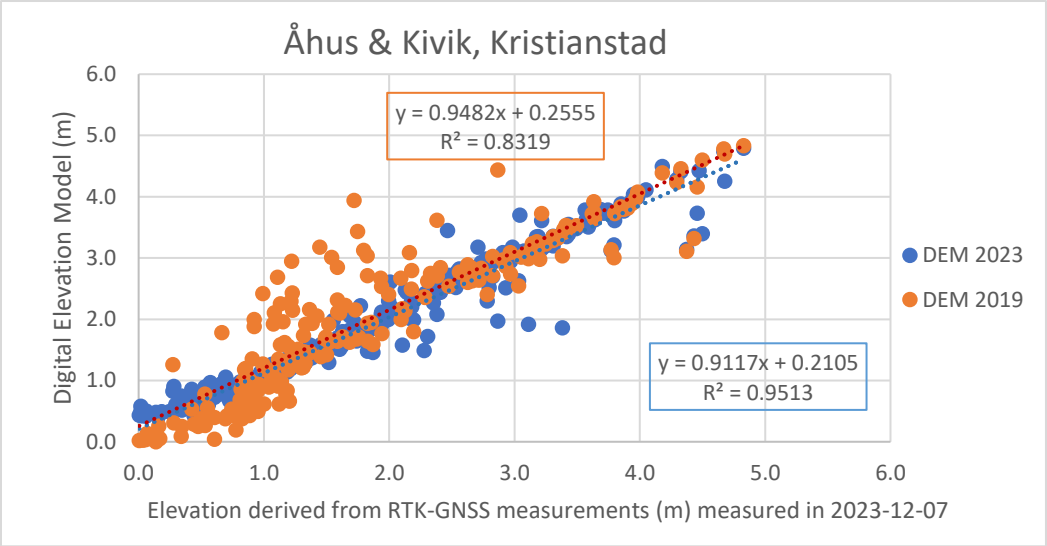

Appendix 25: Scatter Plot depicting the relationship between predicted values (DEM) against observed values (RTK-GNSS) in Åhus & Kivik, Kristianstad. The linear dotted lines represent the best fitted straight line between the predicted and observed values for each year respectively. Ground data measured in 2023-12-07.

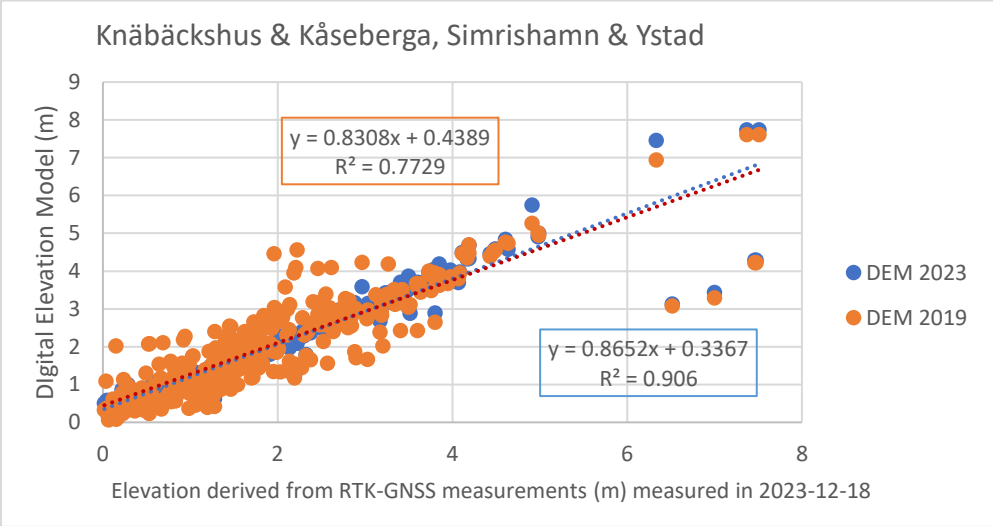

Appendix 26: Scatter Plot depicting the relationship between predicted values (DEM) against observed values (RTK-GNSS) in Knäbäckshus & Kåseberga, Simrishamn & Ystad. The linear dotted lines represent the best fitted straight line between the predicted and observed values for each year respectively. Ground data measured in 2023-12-18.